THE EFFECT OF DILUTE POLYMER SOLUTION ON THE STROUHAL FREQUENCY OF CIRCULAR CYLINDERS

Richard Edward Kell

United States
Naval Postgraduate School

THESIS

THE EFFECT OF DILUTE POLYMER SOLUTION
ON THE
STROUHAL FREQUENCY OF CIRCULAR CYLINDERS

by

Richard Edward Kell

Thesis Advisor: T. Sarpkaya

June 1971

The Effect of Dilute Polymer Solution on the Strouhal Frequency of Circular Cylinders

by

Richard Edward Kell
Lieutenant, United States Navy
B.S., United States Naval Academy, 1963

Submitted in partial fulfillment of the requirements for the degree of

MECHANICAL ENGINEER

from the

NAVAL POSTGRADUATE SCHOOL
June 1971

ABSTRACT

Flow of aqueous solutions of Polyox WSR-301, at a concentration of 25 wppm, was investigated in the cylinder drag transition region of Reynolds numbers. Frequency spectrum and drag force were measured on a circular cylinder (diameter 1 inch). Frequency spectrum, Strouhal frequency and drag force also were measured on circular cylinders in water (diameter 1 and 1-1/2 inch).

The polymer additive did not alter the vortex shedding frequency from that of water at the same Reynolds numbers. As the polymer degrades, a state is reached where concentration, Reynolds number and body size combination become such that the transition occurs in the boundary layer. Transition in the polymer solution occurred earlier than that in the pure solvent. At one Reynolds number, several regimes of flow may be observed as the polymer solution degrades.

TABLE OF CONTENTS

LIST OF FIGURES

ACKNOWLEDGEMENT

The author wishes to express his gratitude to Professor T. Sarpkaya for his invaluable guidance, steady encouragement and ability to impart much more to a student then just technical knowledge. Also, to Professor Houlihan for his constructive supervision throughout this work. The continual assistance of Messrs. K. Mothersell, T. Cristian, G. Baxter, G. Bixler, J. McKay, and J. Beck in constructing and maintaining equipment was greatly appreciated. Finally, to my wife, Susan, for her understanding and help in so many ways.

I. INTRODUCTION

A. PRELIMINARY REMARKS

During the past decade a significant amount of research in the field of fluid dynamics has been carried out on the drag reduction properties of polymer solutions. Various fields of study as diverse as medicine, undersea weapons engineering, petroleum engineering, and agriculture are interested in polymer drag reduction. The motivation behind this interest is the possibility of increasing system performance without increased energy input.

The drag reducing properties of polymer solutions was first noted by Toms in 1948 and still is commonly referred to as the "Toms Effect." A variety of substances exhibit a drag reduction phenomenon to some degree, dependent upon molecular weight and concentration. The most effective polymers have high molecular weight, long molecular chains, and are highly flexible. Generally, these polymers have been effective in very dilute solutions; that is, solutions with less than 1000 parts per million by weight (wppm) of polymer additive.

Extensive reasearch has been performed with internal flows where drag is due primarily to turbulent skin friction, while the study of flow around bluff bodies has received lesser attention because of the complex nature of the body drag forces. The drag force on a bluff body is affected by

boundary layer and wake changes interacting in a kaleidoscope manner in three dimensions. Thus, conclusions reached in pipe flow cannot, with any certainty, be extended to an external body flow situation.

The Reynolds number range in which the flow is studied is important because, here again, significant differences exist between low and high Reynolds flow ranges. Therefore, the results obtained in one range can be very misleading if applied to another range. The study of flows throughout the entire range at Reynolds numbers is an impossible task. Fortunately, only a few finite ranges are of major importance. These are called the critical or transition regions. Of these three or four regions, the one which is of major importance is the transition region from a laminar to a turbulent flow condition.

In order to derive any benefit from polymer drag reduction, the flow around a bluff body must be studied extensively. This simple statement can be reversed into the question: "What equipment should be used to study the flow of dilute polymer solution around a bluff body?" The fundamental problem of how to measure pressure or velocity has an entirely new perspective in dilute polymer solutions. Authors, including Smith, Merrill, Mickely, and Virk [Ref. 1], James [Ref. 2], Wetzel, and Tsai [Ref. 3], have reported anomalous behavior of pitot tubes and thermo-anemometers in polymer solutions. Flow visualization techniques are very useful for a localized investigation of the flow but generally do not provide the

quantitative information necessary. Thus, as an initial step, measurements have to be made from the surface of the body for the transition Reynolds number range. Future development of laser techniques should provide an excellent means of measurements.

B. SURVEY OF PREVIOUS INVESTIGATIONS

The study of the wake behind a cylinder or other bluff bodies has been of interest to researchers for hundreds of years. Leonardo da Vinci sketched a row of vortices behind a cylinder in the 15th century. Strouhal's experiments [Ref. 4] in the 1870's initiated quantitative work in this area. Von Karman's work, early in this century, on the stability of vortex streets' relationship to drag stimulated a preponderance of experimental and theoretical work in this field. To help summarize this vast quantity of literature, several excellent reviews have been published, including Goldstein [Ref. 5], Linenhard [Ref. 6], Morkovin [Ref. 7], Wille [Ref. 8], and Marris [Ref. 9].

The wake behind a circular cylinder can be classified into various regimes of flow with each region displaying its own characteristics. Lienhard [Ref. 5] and Morkovin [Ref. 7] presented similar classifications based on Reynolds number. A combination of the two presentations is shown in Fig. 1. The first noticeable change from unseparated flow is the Appearance of fixed Föppl vortices in the range of Reynolds numbers from 5 to 10. Somewhere between a Reynolds number of 10 and one of 40, the laminar wake becomes unstable and

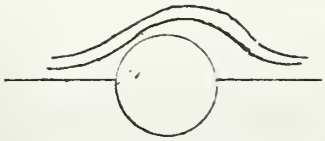

Re<5

REGIME OF UNSEPARATED FLOW.

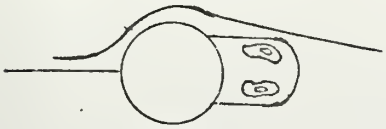

3-5<Re≤30-40
LAMINAR: STEADY IN PRACTICE,
UNSTABLE UNDER ARTIFICIAL EXCITATION.

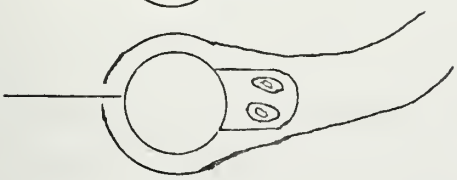

30-40<Re<80-90
LAMINAR WAKE INSTABILITY, SHEDDING
GOVERNED BY WAKE INSTABILITY.

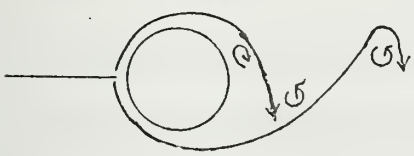

80-90<Re<150

PERIODICITY GOVERNED BY VORTEX
SHEDDING.

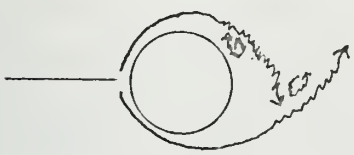

SUBSCRITICAL: 150-300<Re<10-13 $\times 10^4$
TRANSITION TO FULLY TURBULENT VORTEX
STREET, FORWARD PROGRESSION OF TURBU-
LENCE AND INCREASING 3-DIMENSIONALITY,
NEARLY CONSTANT STROUHAL NO., MODERATE
SENSITIVITY TO FREE STREAM TURBULENCE
AND SURFACE ROUGHNESS.

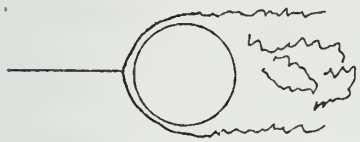

CRITICAL: 10-13 $\times 10^4$<Re<3.5 $\times 10^6$
LAMINAR BOUNDARY HAS UNDERGONE TUR-
BULENT TRANSITION, NARROWER WAKE,
NO VORTEX STREET, STRONG 3-DIMEN-
SIONALITY, STRONG SENSITIVITY TO FREE
STREAM TURBULENCE AND SURFACE
ROUGHNESS.

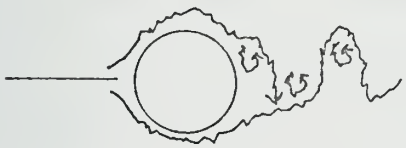

TRANSCRITICAL: 3.5 $\times 10^6$<Re<(?)
TRANSITION TO TURBULENT BOUNDARY ON
THE FRONT FACE OF THE CYLINDER,
RECOVERY OF PRONOUNCED PERIODICITY
CORRESPONDING TO MEDIUM WIDTH OF
WAKE.

Figure 1. REGIMES OF FLOW AROUND A
CIRCULAR CYLINDER

the first appearance of the vortex street at Reynolds numbers above 40 is a result of this instability [Ref. 9]. As the Reynolds number is increased, the wake and the vortices continue to change up to a Reynolds-number range of 1×10^5 to 3.5×10^6, called the transition or critical range, where the boundary layer changes from laminar to turbulent. In this region, the wake narrows, no vortex street is apparent, there is increased three dimensionality, no predominent shedding frequency is apparent, and a strong sensitivity to free-stream turbulence and surface roughness develops. Above Reynolds numbers of 3.5×10^6, Roshko [Ref. 10] reported the re-establishment of a vortex street with a higher Strouhal number (approximately 0.267).

Roshko (1961) presented a plot of both C_d and 1/St versus Re, which portrays the importance of eddy shedding frequency on drag. This plot, same as used by Lienhard, is shown in Fig. 2. The 0.22/St relationship is used to shift the 1/St curve as close as possible to the drag curve. Delany and Sorensen [Ref. 11] also showed this effect using data obtained at Ames Research Center.

Using this similarity, Roshko [Ref. 12] and [Ref. 13] demonstrated how C_d and St are related. This analysis made the important point that not only lift but much of the drag might be eliminated if vortex action could be inhibited. To inhibit vortex formation, Roshko used a splitter plate which obstructed vortex formation and eliminated the extreme back pressure coefficient. Results of this experiment are shown

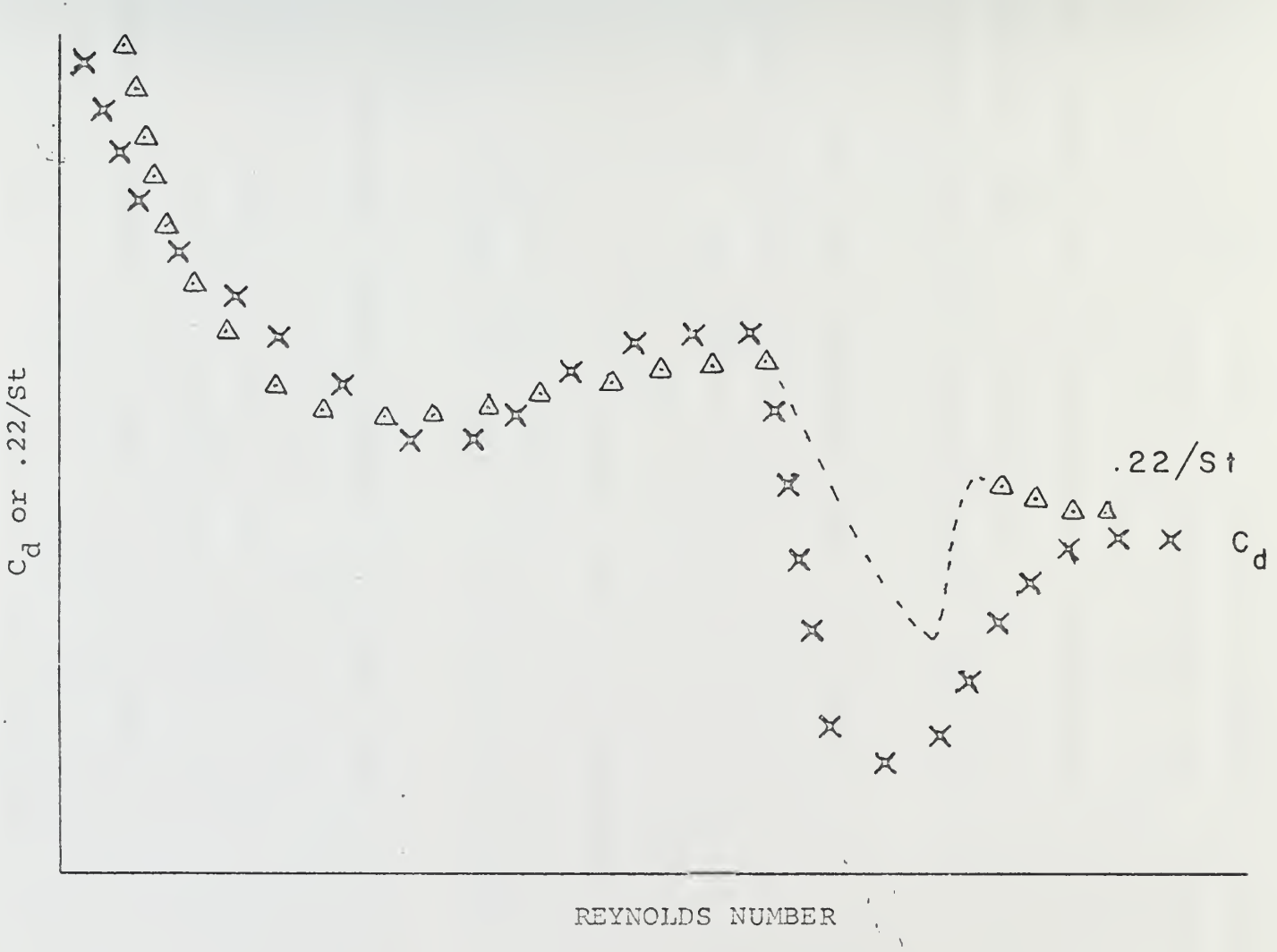

Figure 2: C_d and St VERSUS Re

in Fig. 3. A decrease in drag of almost one-third was obtained by use of a splitter plate.

The primary complication noted in all regimes of flow is the three-dimensional aspect of vortex shedding and wake structure. Gaster [Ref. 14] reported shedding in spanwise cells at Reynolds number of approximately 100. In each cell the shedding was regular and constant but between the cells the shedding was not continuous. Experimental studies of Humphreys [Ref. 15] and Macovsky [Ref. 28] dealt with three-dimensionality in a Reynolds number range from 10^4 to transition.

In his paper, Humphreys [Ref. 15] discussed the effect of three-dimensional vortex motion on average force and boundary layer flow. The random fluctuation of mean drag was the first effect noted. This fluctuation caused changes in drag by as much as 15%, so that any valid C_d measurement must be a time-averaged value. This phenomenon was also noted by Bishop and Hasson [Ref. 16] in conjunction with channel side effects.

Humphreys mentioned another problem concerning cylinder mounting in the test section. Here the type of mounting played a predominate role in the location of the transition region. Humphreys hypothesized that the change in end geometry caused flow changes along the entire length of the cylinder which affected the entire vortex shedding mechanism. Another plausible explanation of this phenomenon can be based on the vibration of the cylinder. Wehrman [Ref. 17] shows

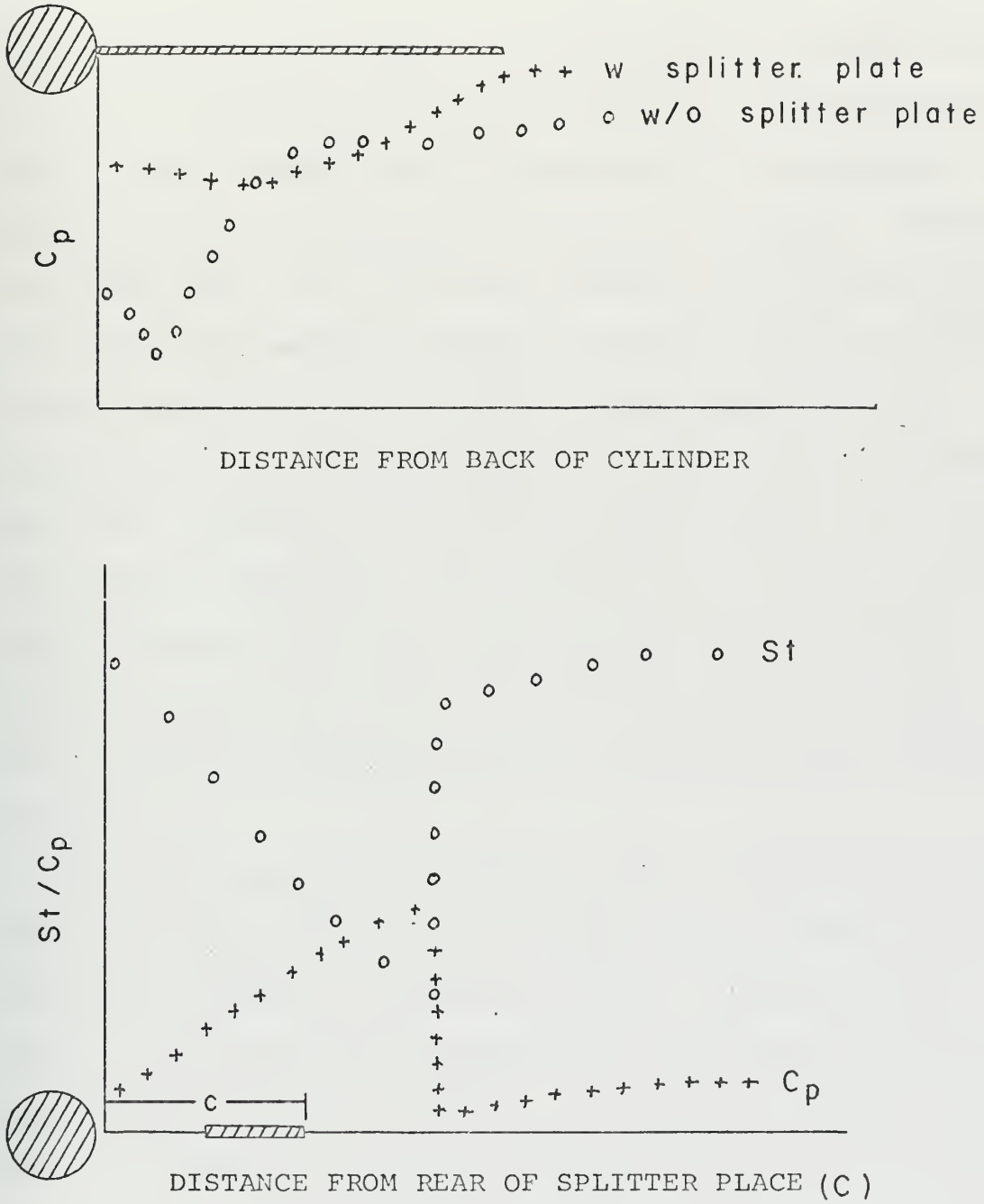

Figure 3: EFFECT OF SPLITTER PLATES [Ref. 6]

that for cylinders at low Reynolds number (less than 350), an external vibration stabilizes the transition region. Bishop and Hasson [Ref. 16] showed a decrease in mean drag for a driving frequency above the critical frequency. These authors also considered the effect of synchronization between cylinder and wake, hysteresis based on increasing or decreasing frequency, and frequency demultiplication, a term used to describe integral multiples of Strouhal frequency. Humphrey's data shows that for a cylinder mounted with both ends free, the transition Reynolds number was higher than the one with one end fixed. One can assume that the free-free case responded to vibration to a greater extent than the fixed-free case. Similarly, on the NPS water tunnel, the fixed-fixed case. Therefore, the transition region was extended for the fixed-fixed case. Vibration studies are limited in number at this point and a great deal of further research would have to be conducted prior to reaching any firm conclusions.

The last and most significant point in Humphrey's paper [Ref. 15] concerned the cell or wave pattern observed by attaching threads at cylinder surface. The cell (Fig. 4) pattern represented an intermediate state which consisted of alternating regions of laminar and turbulent boundary layer flow. The threads caused an earlier initiation of transition and a broadening out of the transition region. It is well known that surface roughness lowers the initiation of transition (see Ref. 5, p. 433), and in this case, the presence of the threads acts as a tripping wire. The formation of these

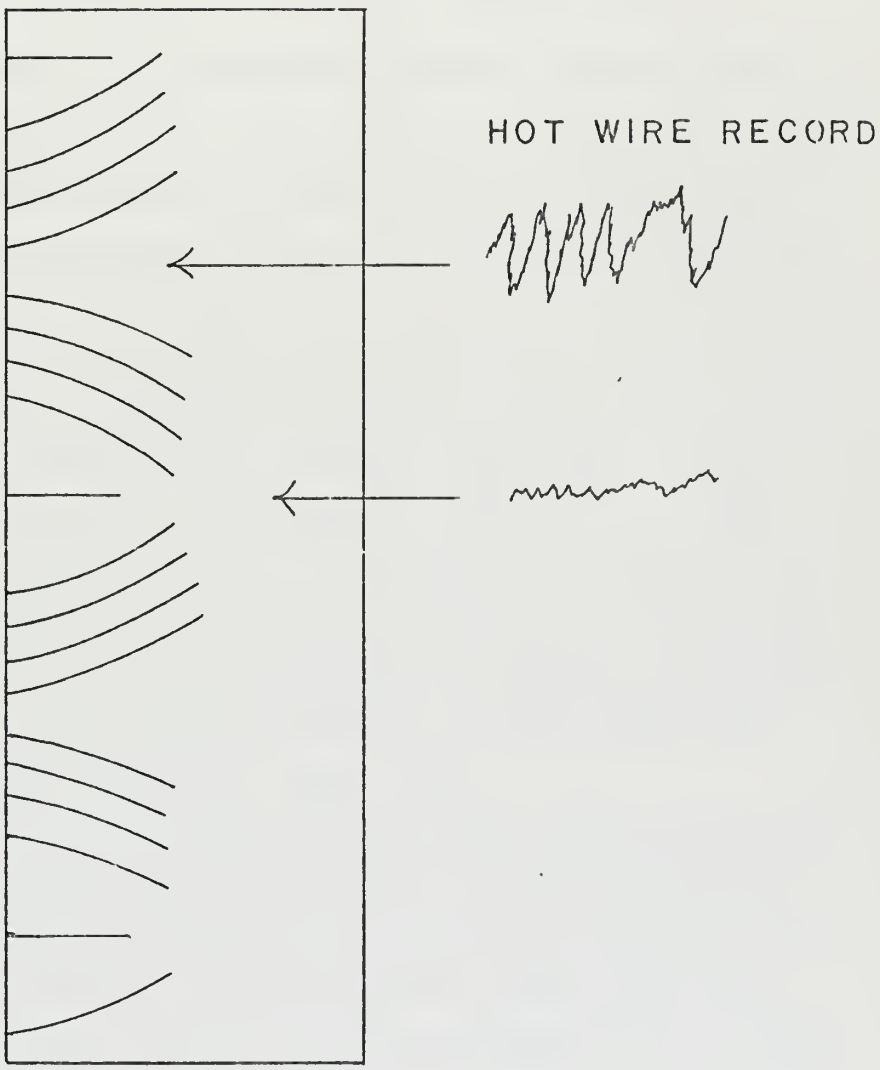

Figure 4: THREADS SHOWING SPANWISE CELL STRUCTURES AT CRITICAL REYNOLDS NO. [Ref. 13]

cells is the first sign of the development of transition at critical Reynolds number.

Gerrard [Ref. 18] conducted a study concerning the three-dimensional structure of the wake of a circular cylinder. It was determined that the modulation of the hot wire signals is a result of the flapping of the wake, and at Reynolds number (R=235) laminar and turbulent vortices occur at the same time behind the cylinder in a spanwise direction. Thus, experimental results based on a two-dimensional model must be interpreted and discussed with three-dimensional effects in mind.

The study of drag reduction in dilute polymer has a very short history when compared to cylinder wake study. The "Toms Effect" was initially reported in 1948 by B. A. Toms but very little was done in this field until the 1960's when several investigators experimented with a variety of polymers in water solution. An excellent survey of this field was presented by Sarpkaya and Rainey [Ref. 19].

The phenomenon of drag reduction by dilute polymer solutions is related to the molecular nature of the polymer in solution. In some manner, the long chain, large size molecules (50,000 times the size of a water molecule) act to aid in the dissipation of energy in the flow.

Patternson [Ref. 20] classified the major theories concerning the polymer drag reduction as follows:

1. Aggregation Theory

Aggregates of polymer molecules retard the intensification of shear layers by an exchange of momentum in the

radial direction. These aggregates stretch out in high shear regions producing an effect similar to the one described by Humphreys [Ref. 15], due to the presence of threads on the cylinder.

2. Anistropic Viscosity Theory

Elongated polymer coils align themselves with the direction of shear and reduce the transfer of momentum normal to the direction of shear. Therefore, the fluid is assumed to have two viscosities, one in the direction of shear (low) and one normal to it (high).

3. Viscoelastic Theories

a. Polymer coil possesses a characteristic relaxation time causing a solid-like behavior for processes with a shorter time scale.

b. The polymer molecule can act as an elastic body and absorb, store, and release energy depending on the influence of the surrounding medium.

4. High Effective (Tensile) Viscosity Theory

In this theory, the high effective viscosity of a dilute solution in an irrotational strain field is directly related to drag reduction and this high viscosity is the result of large polymer-molecule deformations.

A dual explanation of the drag reduction phenomenon was presented in Ref. 19. The first part was based on the concept of roughness elements in the boundary layer or attached to the wall, where the elements were the polymer molecules. The second part conjectured that it is specifically the

finite critical shear wave spped which is the fundamental property that imparts a significant change in the characteristics of the flow. As a result of this finite shear wave speed, a hydro-polymeric boundary layer results and transition characteristics are controlled by the hydro-polymeric boundary layer.

The theories just presented are general areas of agreement between different researchers. These theories provide a basis for aditional research and will continually be refined, combined, accepted, or rejected as additional information is obtained.

Sarpkaya and Rainey [Ref. 19] stated that two distinct types of transition occur in dilute polyox solutions. The first is a continuous transition similar to that noted on roughened cylinders. The second is an actual drag "crisis" or "tripping" of the boundary layer at a well defined flow condition at a constant percentage of degradation. The graphs for these conditions have been replotted in Fig. 5 from Ref. 19 for the one-inch cylinder in a 25 wppm polymer solution.

Very little research has been reported on vortex shedding in dilute polymer solutions with the exception of papers by Kudin, Kalashinskov and Gadd. Kudin and Kalashinskov [Ref. 21] studied the vortex shedding at Reynolds number below 400 with a hot-wedge anomometer. The frequency was obtained by comparing the Lissajous figures from the thermo-anomometer and a known frequency oscillator. The authors

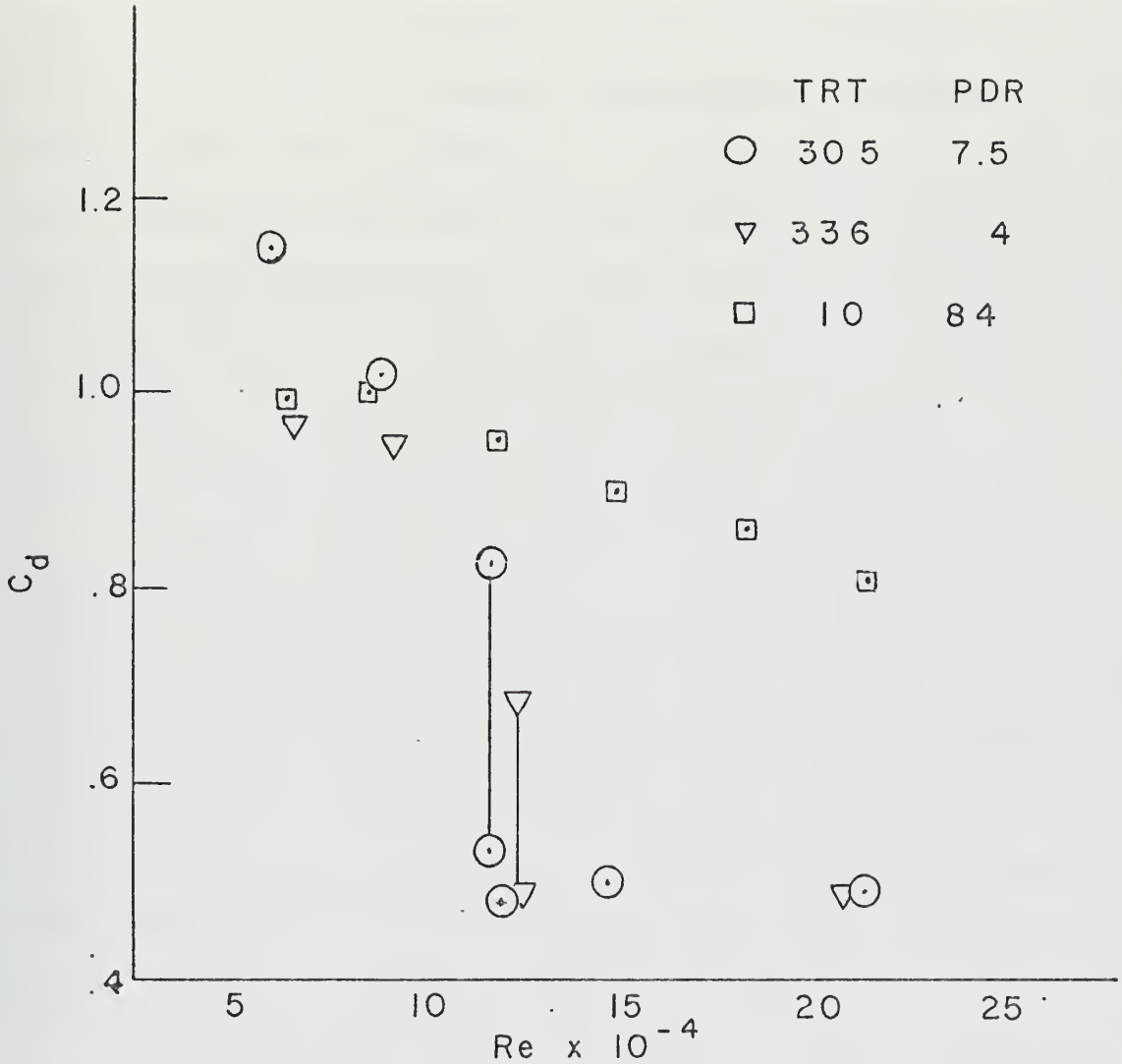

Figure 5: 25 WPPM CRITICAL C_d TRANSITION
1 INCH DIAMETER CYLINDER

found that the frequency obtained in polymer solution was lower than that for the Newtonian fluid. Gadd [Ref. 22] tested several polymers at a Reynolds number of approximately 240 and reported the greatest change in Strouhal frequency ocurred when Polyox WSR-301 was used. Polyox in concentrations up to 40 wppm produced a much lower shedding frequency. Gadd stated that the polymer inhibited the breakdown of the vortex street into turbulence. Below a concentration of 10 wppm, no change was noted in the shedding frequency. In another experiment, Gadd [Ref. 23] demonstrated that Polyox WSR-301 in concentrations up to 90 wppm made it more difficult to stretch a vortex. Therefore, this could delay the breakdown of laminar non-linear oscillations into turbulence.

Genstill [Ref. 24] reported no change in Strouhal number or oscillating forces on a semi-submerged circular cylinder in 100 wppm 200 wppm solutions of WSR-301. The data was obtained by moving the cylinder through the solution, thus the polymer did not degrade to any appreciable extent. These results are consistent with [Ref. 10] where fresh solutions (85% drag reduction for pipe flow) showed little change in Cp or C_d when compared to water.

The important fact that emerges from the preceding observation is the multiplicity of the mechanisms that lead to turbulence and the unavailability of disturbance input information.

C. OBJECTIVES OF THE PRESENT INVESTIGATION

The objectives of this investigation were divided into two parts: The first consisted of the testing of two cylinders in water to facilitate equipment setup and to check on the reliability of the results. The second involved the study of the effects of dilute polymer solutions on vortex shedding behind a one-inch cylinder at Reynolds numbers limited to the range before, during, and after the drag-crisis region [Ref. 19]. The periodicity of shedding was used to indicate if the drag crisis is confirmed to a small Reynolds number range as indicated by the drag coefficient curves.

II. EQUIPMENT AND TEST PROCEDURE

A. EQUIPMENT

1. NPS Water Tunnel

The experiments were performed in a recirculating water tunnel (Fig. 6) with a capacity of approximately 500 gallons. The test section was four inches wide, eight inches high, and 16 inches long. The velocity of the fluid in the test section varied from 5 to 25 fps. A low-rpm, high capcity, 14-inch-diameter-discharge centrifugal pump was used to circulate the fluid. Three flow straighteners provided a testsection velocity profile which remained uniform from 0.5 to 7.5 inches with a standard deviation of 1.8%.

Associated quipment include a 150 gallon stainless steel storage tank, a recirculating pump and filter system, and a 15-gallon head tank.

2. Circular Cylinders

Plexiglass cylinders (Fig. 7) of 1-1/2 inch and 1 inch were used for the frequency studies. The cylinders were mounted through the plexiglass walls of the test section with an "0" ring seal. This seal allowed 360 degree rotation of the cylinders.

Fluctuating pressure and local pressure measurements were made on the surface of the cylinder through a small bore hold (1/32 inch), drilled radially from the cylinder surface to a larger (1/8 inch) hole drilled axially from the

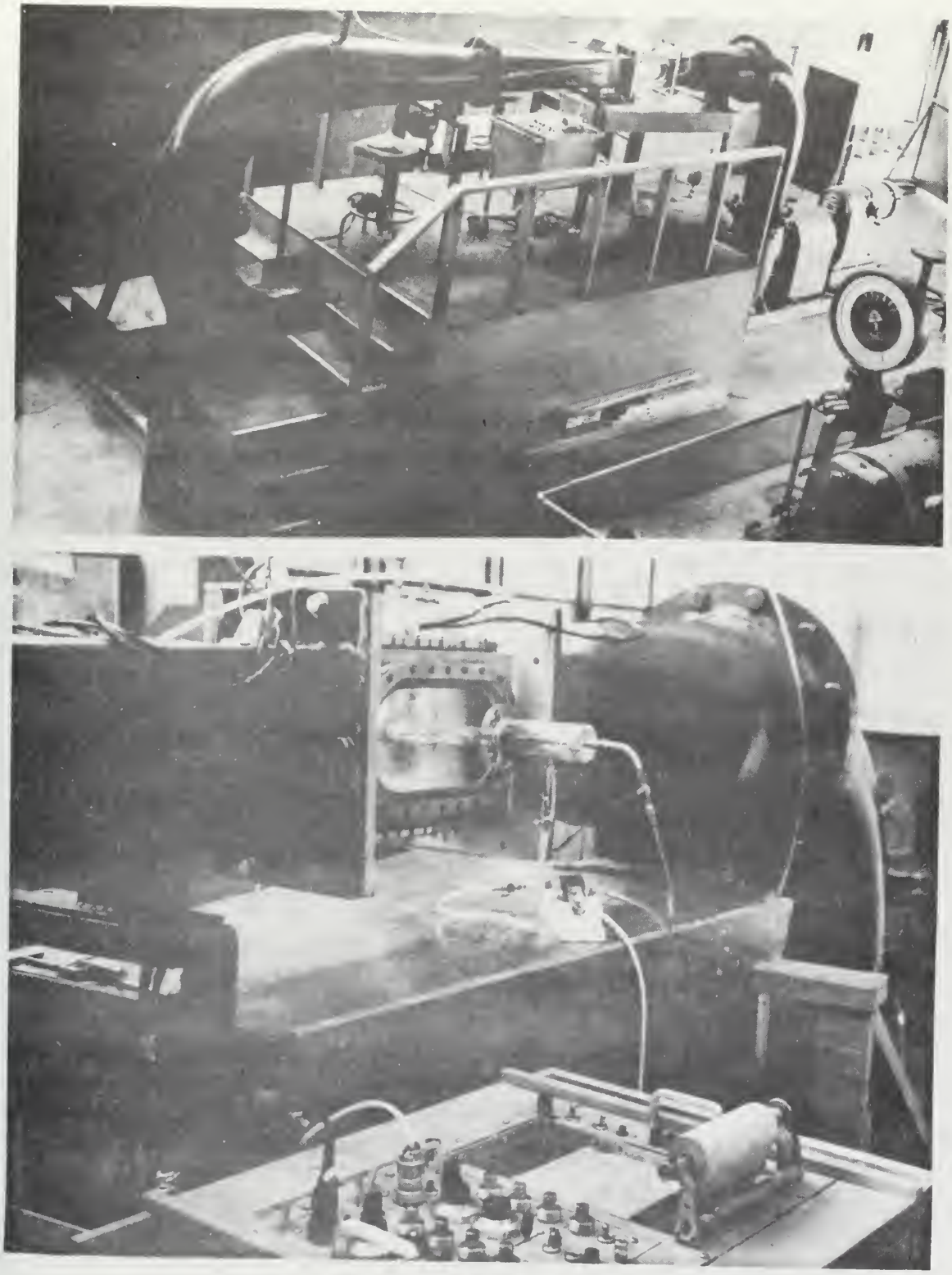

Figure 6: NPS WATFR TUNNEL

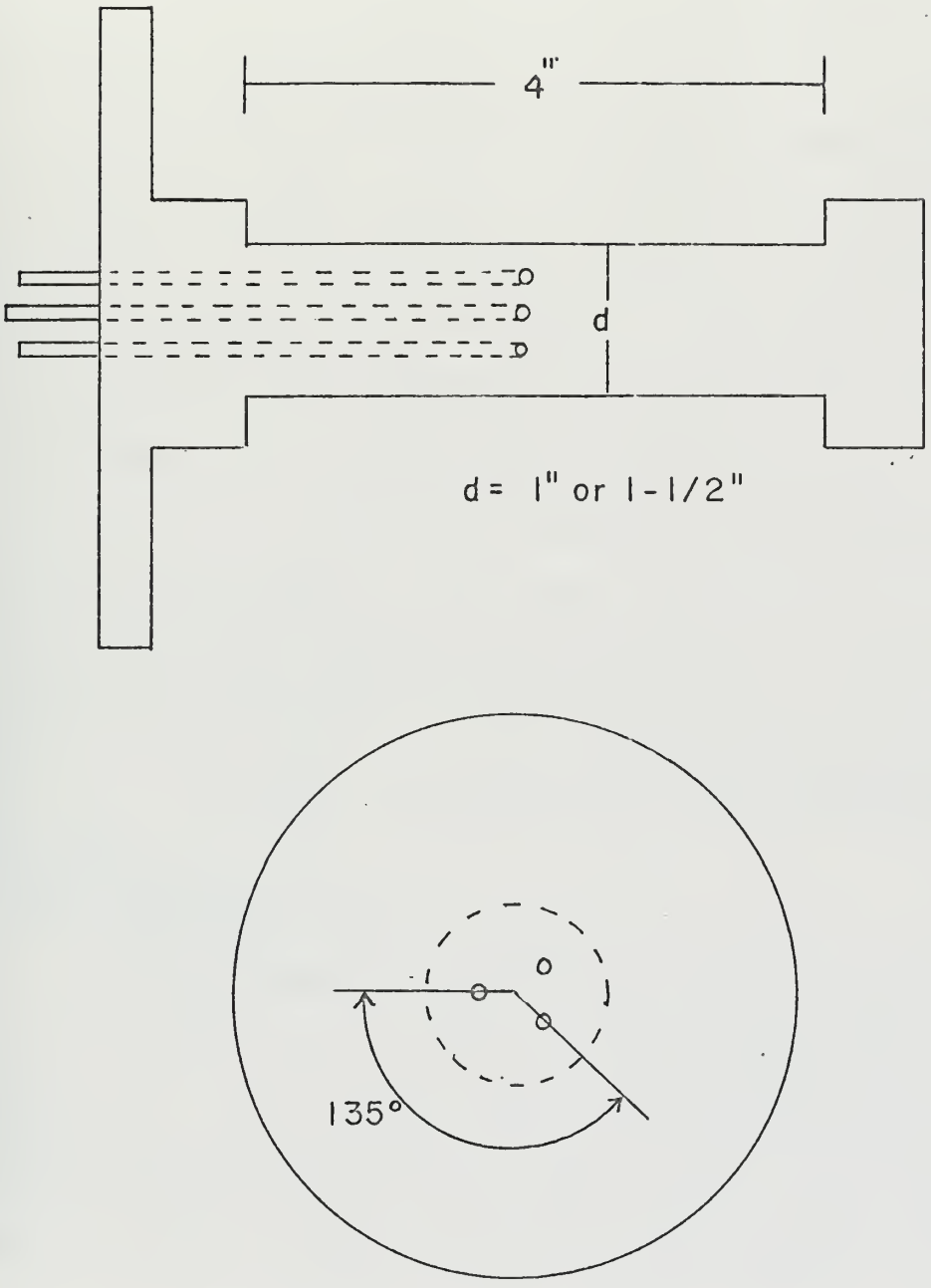

Figure 7: PLEXIGLASS CYLINDER

cylinder end. Small brass tubes were tapped into the 1/8 inch holes to be used as pressure taps on the ends of the cylinders. Each cylinder had 3 bore holes at 0°, 135°, and 225°, located approximately 2 inches from the end of the cylinder (Fig. 7). Static pressure was measured at the entrance of the test section with a wall tap.

An aluminum one-inch cylinder was used for the combined frequency-drag studies. The cylinder was fixed in one test section wall and extended through the other wall and was mounted rigidly in a cantilever beam system. A water-tight plexiglass box enclosed the entire system (Fig. 8). The cylinder contained two small holes (1/32 inch) drilled radially at 0° and 120° for stagnation and fluctuating pressure measurements. Two larger axially drilled holes were mounted with brass tubes for pressure taps. Soft polygon tubing connected these pressure taps to the wall of the water tight box. Pressure transducers were then connected to these wall taps.

3. Instrumentation

The Strouhal number data in water for one-inch and one and one-half inch cylinders was calculated from fluctuating pressure measurements taken at two points, located directly opposite each other $\pm 45°$ from the rear stagnation point. The two pressure leads (at equal length) were attached to a Sanborn Differential Pressure Transducer (Model 267BC). The output of the pressure transducer was fed into a dual channel Hewlett-Packard (H-P) Strip Chart Recorder.

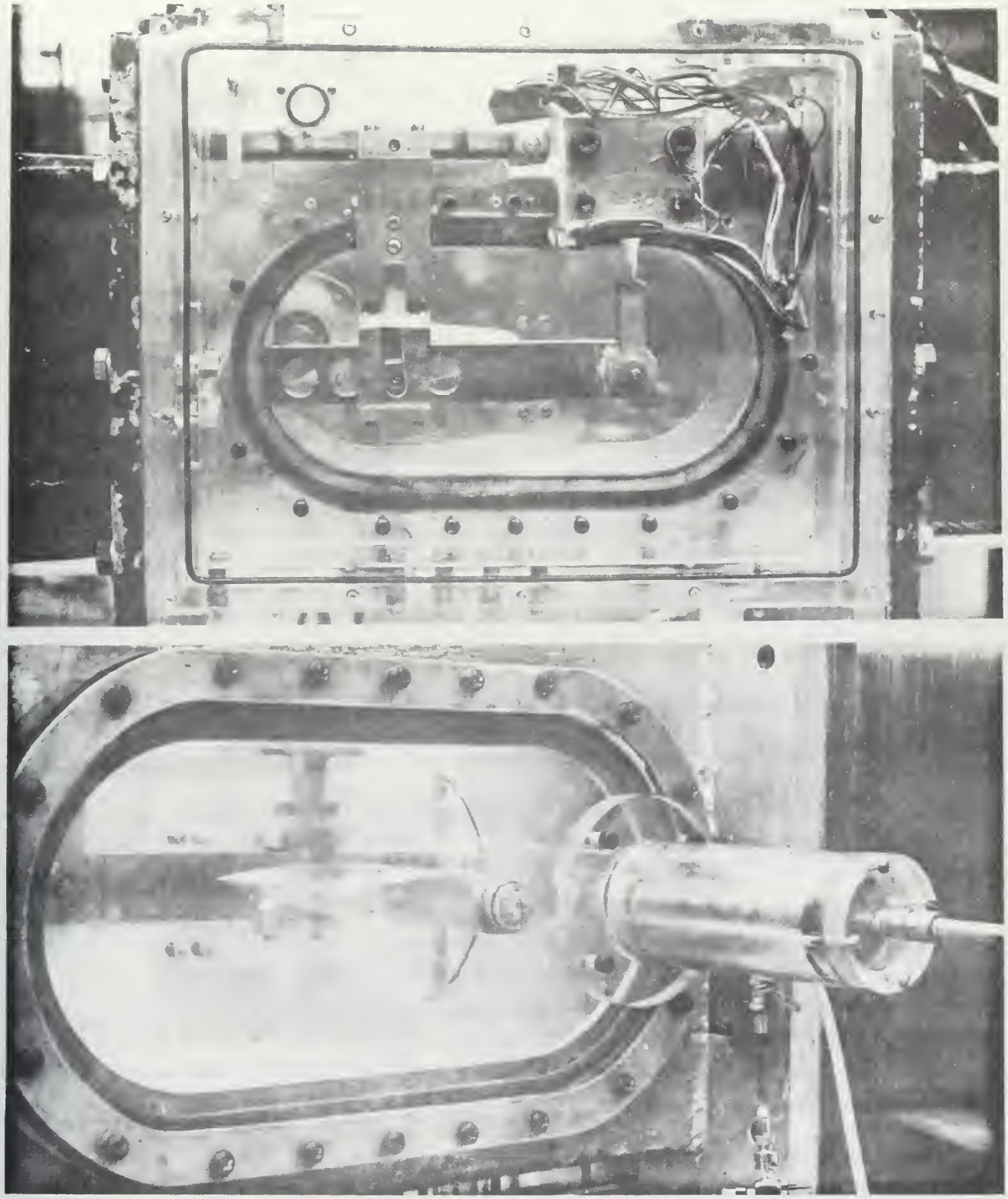

Figure 8: DRAG FORCE MEASURING APPARATUS

A Mansanto Counter (Model 5326B) was added later to check initial data. Kaman (Model K1500 Pressure Transducers were used as an additional check on the Sanborn Transducer. The schematic diagram for the system is shown in Fig. 9.

Frequency spectrum measurements were made using only one port at 60 degrees from the rear stagnation point. A pressure lead from this port was connected to one side at the Sanborn transducer. The other side was left open to the atmosphere. The output of the transducer was fed to the H-P recorder (for amplification only), then through a Krohn-Hite (Model 3750) Low Frequency Band Pass Filter. The output of the filter was connected to a H-P 20 second time constant, RMS meter, the DC output of which was connected to a H-P digital voltmeter printer system. This one port arrangement was used on the alumiunum cylinder for Strouhal frequency measurements. Additional equipment included a tape recorder which monitored all unprocessed signals and a PAR Correlator-Fourier Analyzer for frequency checks. A system schematic is shown in Fig. 10.

The drag force acting on the cylinder was measured directly be a strain gage mounted on the cantilever beam. The beam was fitted with a redundant bridge circuit to maximize reliability. All of the bridges used four active strain gages (SR-4). The gages were calibrated, using a static load from zero to twelve pounds, to a H-P Strip Chart Recorder.

4. Turbulent Pipe Rheometer

The turbulent flow pipe rheometer (Fig. 11) consisted basically of a 0.073 inch ID stainless steel pipe connected

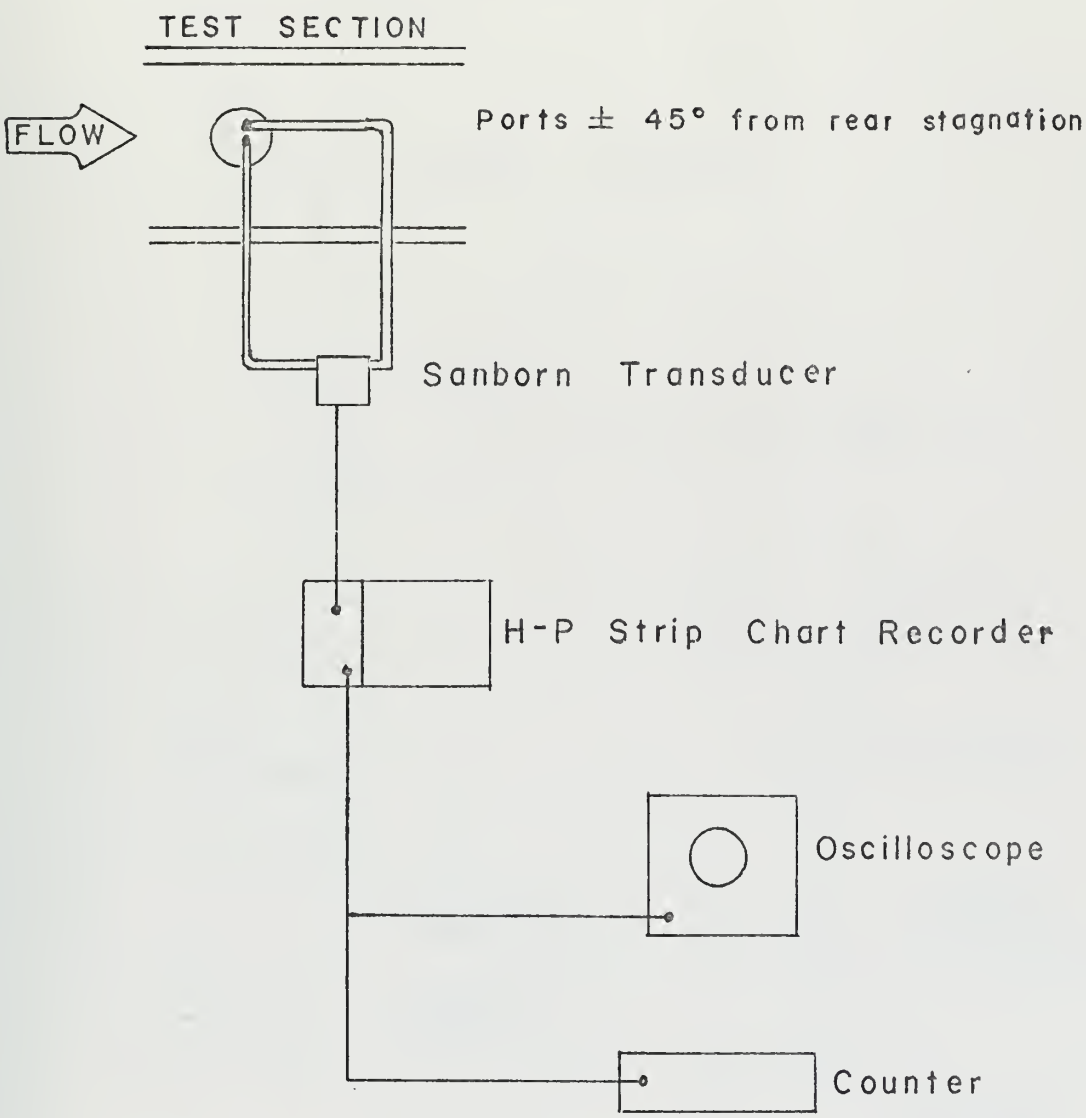

Figure 9: STROUHAL FREQUENCY DATA AQUISITION SYSTEM

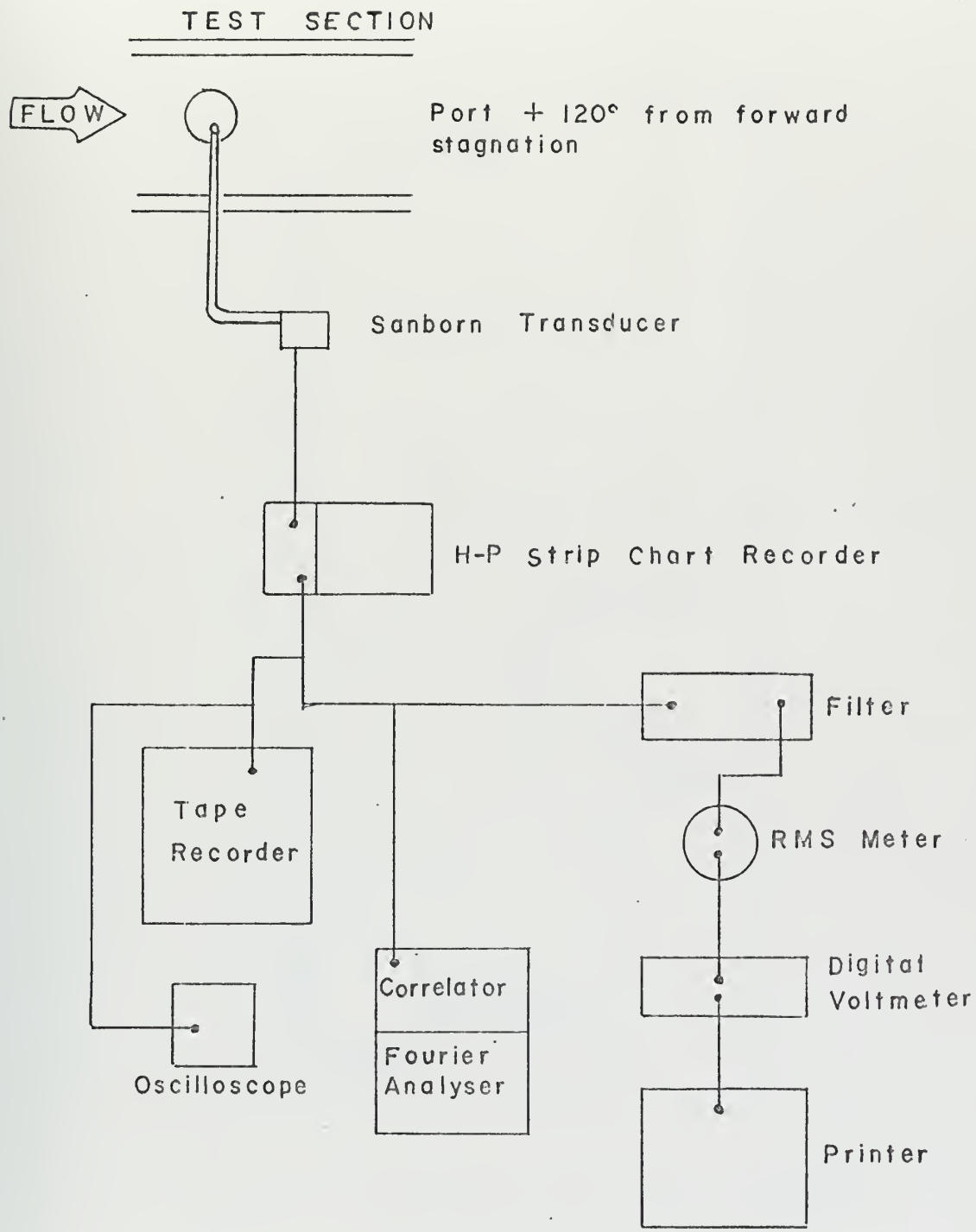

Figure 10: FREQUENCY SPECTRUM DATA AQUISITION SYSTEM

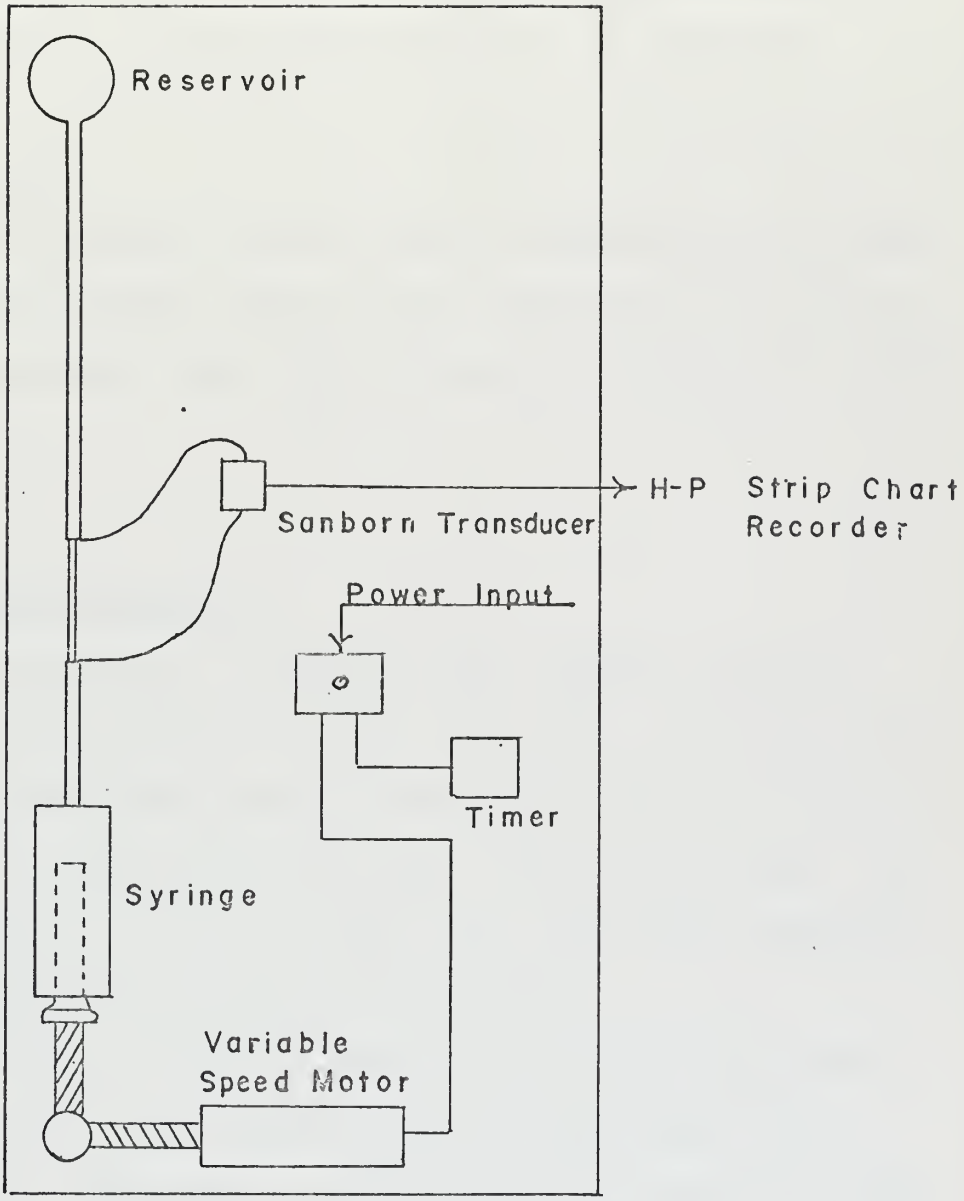

Figure 11: TURBULENT FLOW PIPE RHEOMETER

to a 100cc graduated syringe. The syringe was driven through a worm gear box by a variable speed motor. The pressure drag across the six inch length of the pipe was measured by a Pace Transducer and recorded on a H-P Strip Chart Recorder, while the duration of flow was measured by an electronic timer.

5. Polymer

Polyox (WSR-301), Blend 8051 F, manufactured by Union Carbide, was the polymer used in all experimental runs. WSR-301, a water soluble resin, has a molecular weight of 4×10^6 [Ref. 25].

B. PROCEDURE

1. Rheometer Operation

The syringe was filled from the reservoir as the plunger was slowly lowered to the 120cc level. The motor was started at a preselected speed by manually closing a relay. As the syringe passed the 100cc mark, the electric timer was manually started. As the 20cc mark, the relay was released, instantly stopping the timer and the motor.

The Fanning friction factor for tap water (f_t) was then calculated for the Reynolds number range from 4200 to 5400. This data (Appendix A) established the reference value for the percent drag reduction (PDR) when compared to the friction factors (f) calculated for various polymer solutions.

The polymer solutions were tested in the Reynolds number range of 4800 ± 300. The PDR for each sample of polymer was calculated from the value of the tap water friction factor

corresponding to the Reynolds number of the test. Again, for the purpose of correlating the data, the PDR formula used in Ref. 19 was used in this work.

$$PDR = 100x\ (f_t - f) / (f_t - 64/Re)$$

Tunnel samples were tested prior to the first frequency spectrum run, and after each run. Sufficient sample was withdrawn to allow one flush of the rheometer, and three tests. The same Polymer solution was never used more than once for a PDR test. A PDR was calculated for each test and the three PDR's were then averaged to obtain a single PDR at the end of each run.

2. Preparation of the Polymer

Previous experience [Ref. 26 and 19] proved that the most satisfactory mixing technique was a direct insertion of the dry powder into the circulating water. To accomplish this, the water level was set at the lower one-third of the test section, the pump was started at the slowest speed, and the polymer was slowly fed through a funnel in the tope of the test section. The weight of the dry Polyox was measured to $\pm$ 0.05 gm on a laboratory balance. The total running time (TRT) does not include mixing times which were four minutes or less. The solution was then aged approximately 24 hours before a run was made.

At the completion of a test run, the degraded solution was dumped, the tunnel was flushed twice with water (second filling was filtered for approximately six hours) before

another batch of polymer was mixed. The same procedure as outlined in Ref. 19 was used to chemically treat the tunnel before taking any water data.

3. Cylinder Strouhal Number Measurements in Water

The free stream tunnel velocity was calculated from the measured stagnation pressure of the cylinder being tested. This procedure was used for all experiments in the report.

The Strouhal number was measured on the one-inch-diameter cylinder with tunnel velocities ranging from approximately 7 to 20 fps. Various methods were used to eliminate possible system abnormalities.

The first method, described in the instrumentation section, used two holes $\pm$ 45° from the rear stagnation point. These two pressure ports were connected to a Sanborn differential pressure transducer with soft flexible polygon tubing. The output of the transducer was recorded on a H-P Strip Chart Recorder (Fig. 12). A characteristics frequency was obtained by counting and averaging the cps of the wave form over a three second period.

Hard, non-flexible tygon tubing of the same length was substituted for the soft tube and the tests were rerun to check the influence of the tubing. A wave form very similar to that of the soft tube was obtained (Fig. 13).

A Monsanto Counter was added to the output of the H-P Strip Chart Recorder. The counter agreed exactly with the strip charts, so the recorder pen was bypassed and only the recorder amplifier was used with the counter.

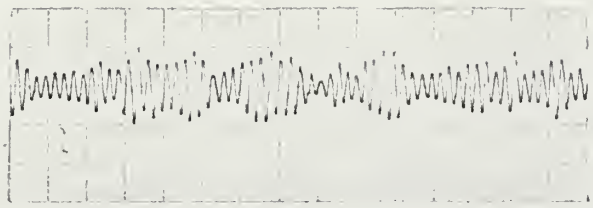

Figure 12: STROUHAL FREQUENCY CHART RECORD, SOFT TUBE

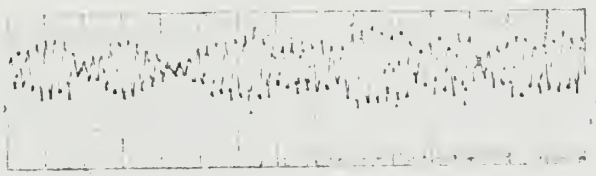

Figure 13: STROUHAL FREQUENCY CHART RECORD, HARD TUBE

In the final test, two Kaman Pressure Transducers were substituted for the Sanborn Transducer. The output of these transducers and associated equipment was amplified and counted on the Monsanto Counter. This check was considered satisfactory since now the fluctuation pressure was being computed electronically, connecting tubing was less than one inch in length as the transducers were isolated from the system vibration.

Measurements on the 1-1/2 inch cylinder were conducted in a free stream tunnel velocity range of 6 fps to 15 fps. The only method used with this cylinder was the same as the first method used on the one-inch cylinder. This method provided results until the 1-1/2 inch cylinder entered the transition region at a Reynolds number of approximately 170,000. In the transition region, a count could not be made on the strip chart. The addition of a counter produced steady frequencies that were dependent only on amplifier gain.

4. Cylinder Frequency Spectrum Measurements

During the second phase of the investigation, frequency spectrum measurements were made. For this series of tests, only the one-inch cylinder was used in polymer and both the one-inch and 1-1/2 inch cylinders were used in water.

Initial checks were made in polymer and water to determine the point on the cylinder where maximum pressure occurred. In water, this point was located at 125 degrees from the forward stagnation point. In 25 wppm polymer solution, the maximum pressure occurred at 110 degrees from the

forward stagnation point. A point was chosen for all tests at 120 degrees from forward stagnation point since readings at this point in polymer and water were less than 1% below the maximum. The above tests were run for a Reynolds number range of 100,000 to 160,000.

Hard tygon tubing was very sensitive to tunnel and building vibration. To reduce this phenomenon, two pieces of soft tube (2 inches long) were attached to either end of the hard tube. With this hook-up, the maximum rms value for exterior vibration between 2 Hz and 135 Hz was 0.05 volts. This was less than 10% of the signal minimum on any run. This combination of soft and hard tubing gave the best signal transfer characteristics with minimum external interference.

The procedure for frequency spectrum spectrum tests in water and polymer solution was not altered once it was established. The band pass filter was set in the band pass mode with high and low cutoffs at the same frequency. The filtered signal was fed to the RMS digital voltmeter, printer system. The RMS value was then printed out at various speeds over a 10 second sample period. The number of printed values varied from a minimum of ten to a maximum of twenty. The filter was then changed to the next higher frequency, and after a delay of approximately 30 seconds another set of readings were taken. A total of 16 frequencies were sampled on every test with concentrated readings near the maximum expected value of rms.

The printed values for each frequency were averaged to obtain a single rms value. Since the digital printer

system output was normalized to the scale setting, each average value of rms was multiplied by the scale setting to obtain the actual rms value. The method described above required the use of the IBM 360 Computer. The data was transcribed from the paper tapes to cards and a program was written to compute and plot the data.

Tests were made in water on the 1-1/2 inch cylinder for Reynolds numbers of 78000, 110,000, 150,000, 180,000 and 210,000. The one-inch cylinder was tested in water at Reynolds number of 72,000, 100,000, and 138,000.

The testing procedure used in the 25 wppm polymer solution varied from that in water since the solution degraded with running time. Two separate series of tests were run with the one-inch plexiglass cylinder, one at Re = 100,000, and the other at Re = 160,000. Each series consisted of 15 tests corresponding to a certain PDR and total running time (TRT). The PDR and TRT are the values at the end of each test. One test book approximately 15 minutes to run. Initially, tests were conducted as close together as possible, due to the rapid change in PDR, but after a PDR of 10% was reached, the tunnel had to run 20 to 30 minutes between tests to show a change in PDR. Tape signals from all runs were also run through the PAR Correlator and Fourier Analyzer to check the frequencies determined by band pass filter method. The correlator analyzer could not be substituted for the band pass system because constant gain changes resulted in an amplitude that had no relationship to other amplitudes.

5. Cylinder Strouhal Frequency and Drag

Frequency spectrum measurements were again taken at a point 120° from forward stagnation. The same procedure used in Part (4) was used for these measurements. Drag measurements. Drag measurements were taken at the same time for correlation purposes.

The test program was as follows:

(a) The one-inch cylinder was tested in water for frequency and drag over a range of Reynolds numbers.

(b) The one-inch cylinder was tested in a 25 wppm solution with frequency measurements taken at Re = 120,000. Drag measurements were made at the same time for Reynolds numbers of 100,000, 120,000, and 160,000. These measurements were taken at various PDR's.

(c) At a value of PDR = 7%, the cylinder was tested over a range of Reynolds numbers with emphasis placed on numbers near the crictical region.

(d) The one-inch cylinder was tested in a 25 wppm solution of Re = 100,000 with drag and frequency measurement taken at various PDR as the solution degraded.

III. PRESENTATION OF DATA

A. EVALUATION OF EXPERIMENTAL ERRORS

The measurements of the stagnation pressure and direct drag were the most critical, since the correlation of the data was based on these measurements. Previous work on the NPS water tunnel has shown that, as the blockage factor increased the stagnation pressure decreased to a value lower than that expected for the fresh polymer solution of concentrations of 50 wppm and larger. All of the following data were taken on the same size cylinder at 25 wppm so that any anomaly due to concentration and blockage factor was kept constant. Error estimates were based on the repeatability of the results in water and polymer solutions. Stagnation-pressure error was estimated to have introduced a relative error of 3%. Drag-force measurements were assumed to have an error of 6%. These errors resulted from calibrations, balance, and zero shift of the recorder and the reading of the recorder chart paper to $\pm$0.2 mm.

The pipe Rheometer had several possible sources of error that included $\pm$0.2 mm recorder reading, $\pm$0.1 second timing error, and $\pm$ 2% error due to the variation of the motor speed during a test run. The above errors, when combined, resulted in an estimated 4% error in PDR reading.

Strouhal frequency measurements had approximately 2% error based on the comparison between different methods of testing.

RMS frequency measurements were averaged over certain time periods at various sample rates and compared with a Fourier frequency analysis of the same signal. This resulted in a 2 Hz error for 30 Hz signal or in a 7% maximum error.

The expected total error is defined as the square root of the sum of the individual errors squared. Therefore the expected total error was estimated at 7% for drag, 3% for Strouhal Number, and 9% for the frequency measurements.

B. STROUHAL NUMBER AND FREQUENCY SPECTRUM MEASUREMENTS IN WATER

1. Strouhal Number for Cylinders in Water

The Strouhal frequency was measured on the one-inch plexiglass cylinder over a range of Reynolds numbers from 5.4×10^4 to 16.7×10^4. As stated in the experimental procedure, three changes were made on the pressure measuring system. First a soft tube then a hard tube and finally two Kaman Hydrophones were used to check for system abnormalities. In Fig. 14, the measurements made with these methods have been compared by plotting Strouhal versus Reynolds number. No noticible difference was observed between the three methods. The constancy of the Strouhal number and the predominant frequency indicated that the cylinder was in a subscritical-flow regime. A representative sample of all the data taken with the one-inch plexiglass cylinder is shown in Fig. 15. A similar plot representing all the data taken on the one and one half inch plexiglass cylinder is shown in Fig. 16 for a Reynolds number range of 7.8×10^4 to 18.4×10^4. At Reynolds numbers above 16.5×10^4, the Strouhal number increased,

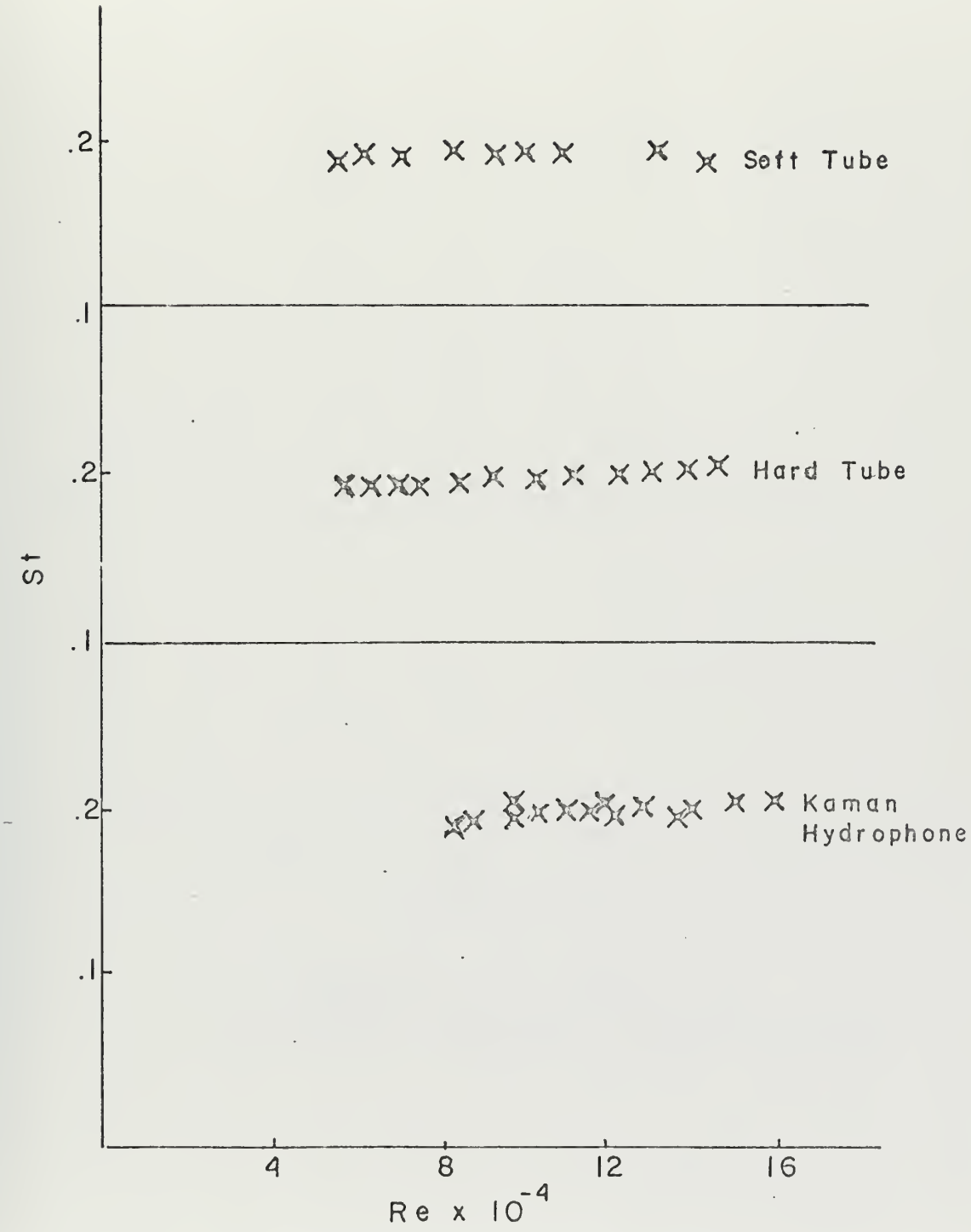

Figure 14: St VERSUS Re
COMPARISON OF DIFFERENT PRESSURE SENSORS

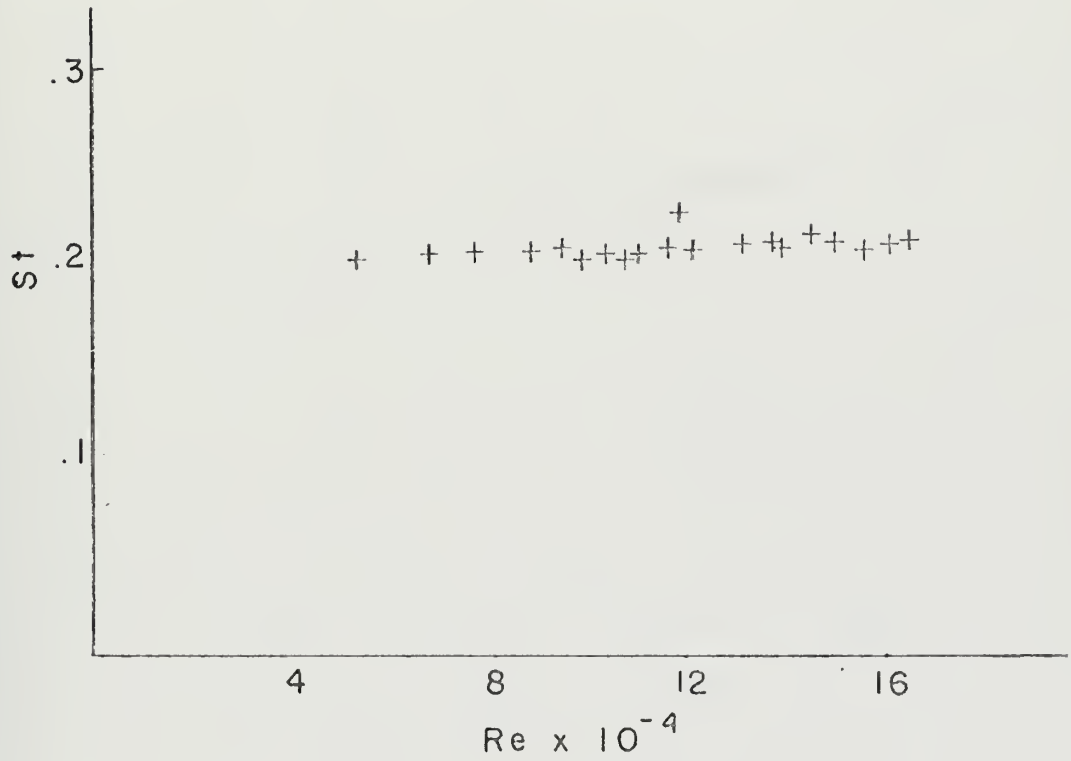

Figure 15: St VERSUS Re
1 IN. DIAMETER PLEXIGLASS CYLINDER IN WATER

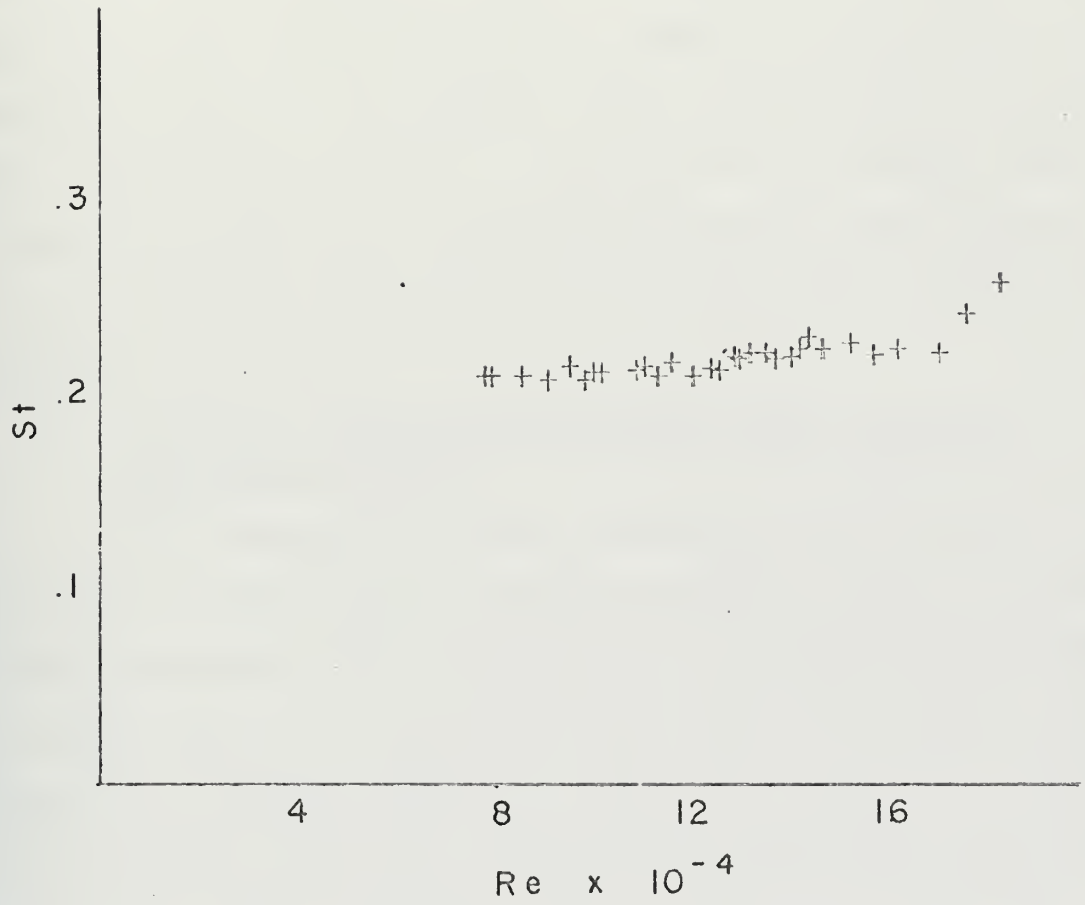

Figure 16: St VERSUS Re
1-1/2 IN. DIAMETER PLEXIGLASS CYLINDER IN WATER

corresponding to a loss of predominant frequency, thus indicating that the one and one half inch cylinder has entered the transition region.

The one-inch aluminum cylinder was tested in water over a Reynolds number range of 5×10^4 to 15×10^4. At Reynolds numbers above 15×10^4 no predominant frequency was noted thus indicating that the cylinder had entered the transition region. A Strouhal number versus Reynolds number plot is presented in Fig. 17. The Strouhal frequency was taken at one port 120° from the forward stagnation point for the aluminum cylinder instead of the two port method used on the plexiglass cylinders.

2. Frequency Spectrum Measurements with One-Inch Cylinders in Water

All frequency spectrum measurements were taken at the same point, 120° from the forward stagnation point. As stated in the discussion of the procedure, all spectrum measurements were made using the bandpass-filter method and each run was checked by a Fourier Analysis on the PAR equipment. Three spectrums were taken with the one-inch plexiglass as shown in Fig. 18 for Reynolds numbers of 7.2×10^4, 10×10^4, and 13.8×10^4. Figure 19 illustrates a typical Fourier Analysis for a Reynolds number of 10.0×10^4. Both plots show a maximum amplitude at 30 Hz which corresponds to the Strouhal Frequency recorded previously. The frequency spectrum for the one and one half inch cylinder for Reynolds numbers of 7.9, 15, 24.6×10^4 are grapher in Fig. 20. The frequencies of the maximum amplitudes for Re = 7.9 and 15×10^4 again correspond

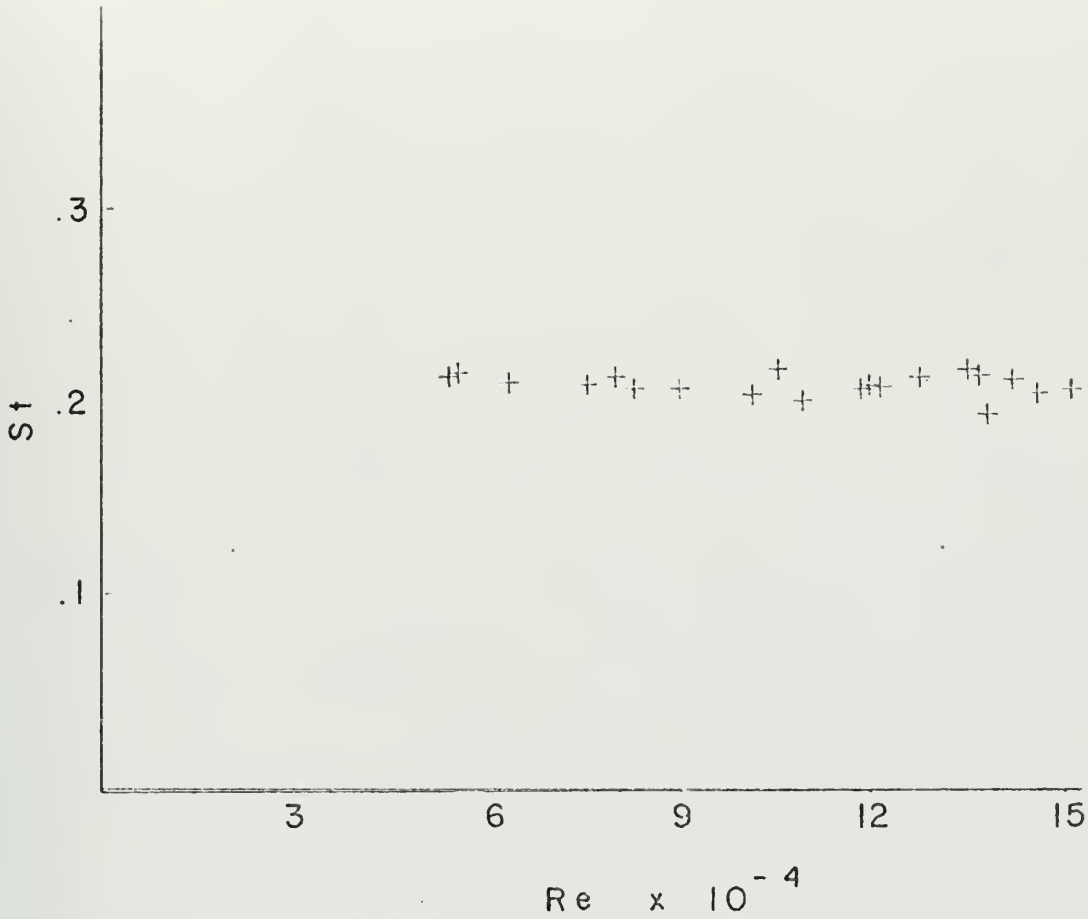

Figure 17: St VERSUS Re
1 IN. DIAMETER ALUMINUM CYLINDER IN WATER

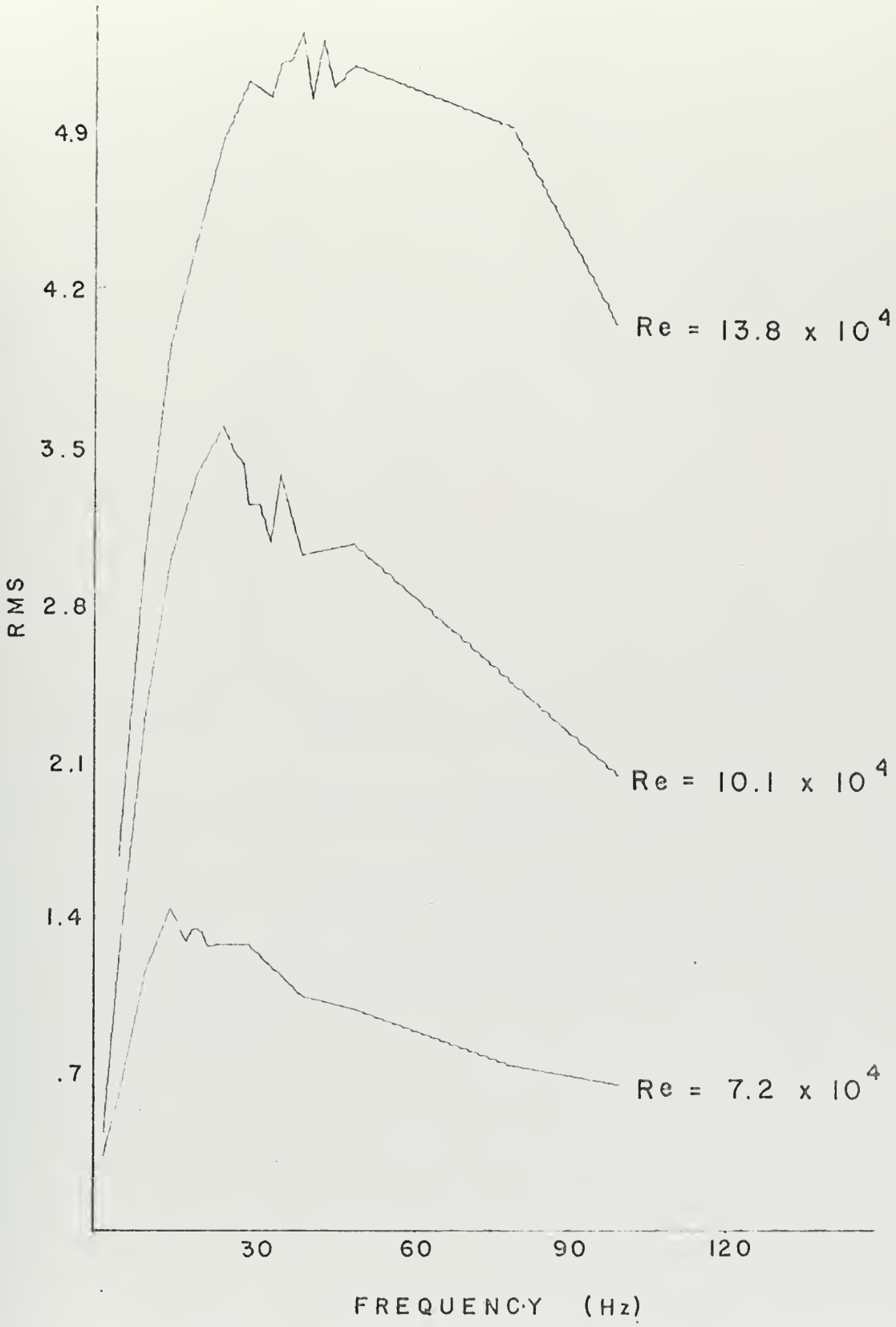

Figure 18: RMS VERSUS FREQUENCY
1 IN. DIAMETER PLEXIGLASS CYLINDER IN WATER

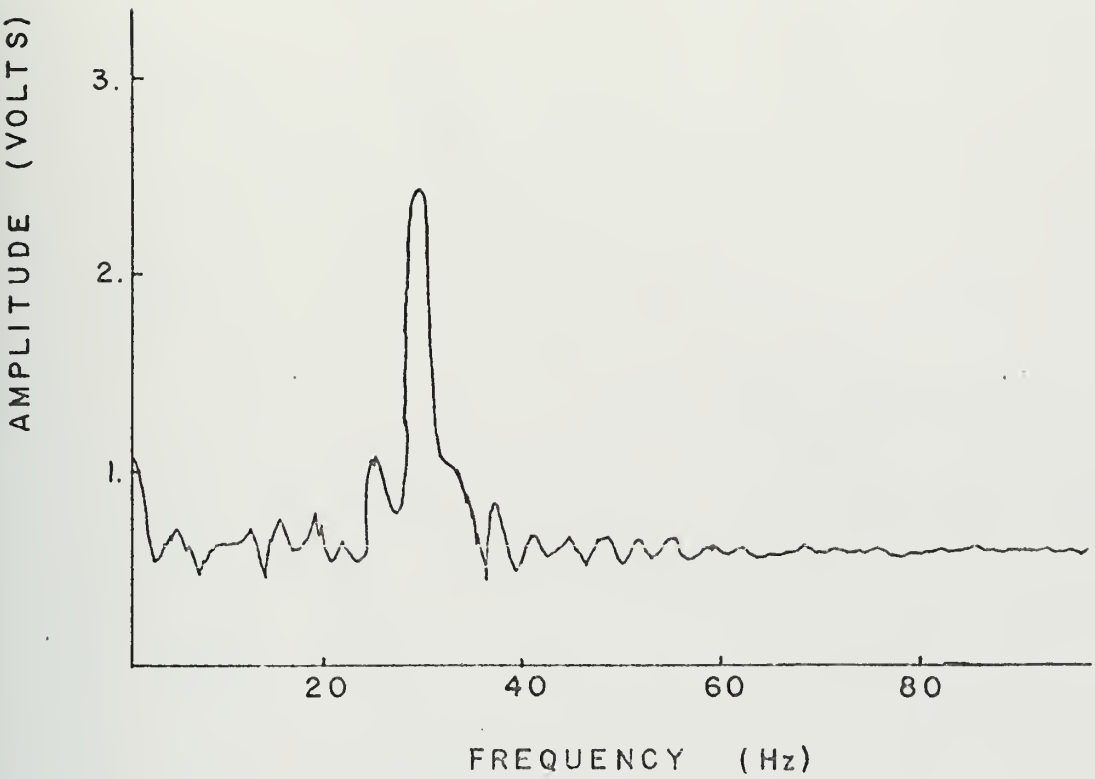

Figure 19: AMPLITUDE VERSUS FREQUENCY 1 IN. DIAMETER PLEXIGLASS CYLINDER WATER ($Re = 10x10^4$)

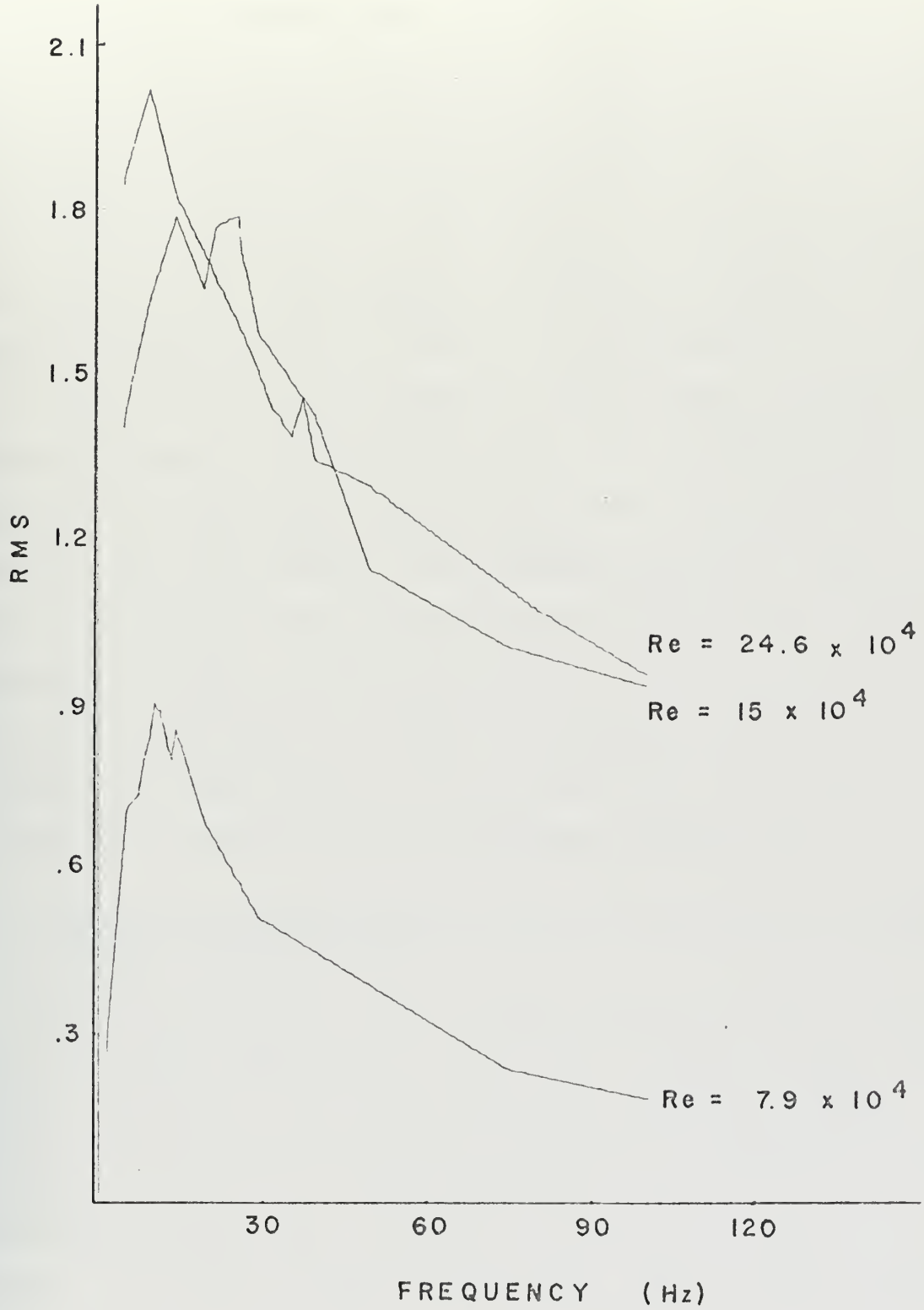

Figure 20: RMS VERSUS FREQUENCY
1-1/2 IN. DIAMETER PLEXIGLASS CYLINDER IN WATER

to the Strouhal frequencies. For Reynolds numbers above 24.6×10^4, the flow is well into the critical regime and has lost all the predominant frequencies except for a very low frequency of 10 Hz. The pressure waveform in this case appeared on the oscilloscope as a low frequency wave modulated with high frequencies. The aluminum cylinder was tested at three Reynolds numbers of 10, 12 and 16×10^4 as shown in Fig. 21. Again the frequencies correspond to the Strouhal frequency at Reynolds numbers of 10^5 and 12×10^4. At Reynolds numbers above 16×10^4 the spectrum has flattened out at high frequencies and a predominant low frequency peak has appeared. The only change between the mounting of the plexiglass and the aluminum cylinder was the end conditions. The plexiglass cylinder was fixed in both test section walls while the aluminum cylinder was only fixed on one end with the other end open to a reservoir housing the drag mechanism (Appendix B).

C. FREQUENCY SPECTRUM FOR THE ONE-INCH PLEXIGLASS CYLINDER (25 wppm CONCENTRATION)

Two tests were run with the one-inch plexiglass cylinder for a Reynolds number of 10×10^4, in a 25 wppm polymer solution. Initially, the polymer solution (85% PDR) behaved similar to water but as the PDR changed, the entire frequency spectrum changed also. Figures 22 and 23 illustrate the change of frequency spectrum with PDR. The minimum frequency spectrum was almost flat and was observed at a PDR of 20%. The return to water-like behavior was accomplished by degrading the polymer by pumping. This phenomenon of the frequency-spectrum change can be shown by plotting RMS versus PDR for

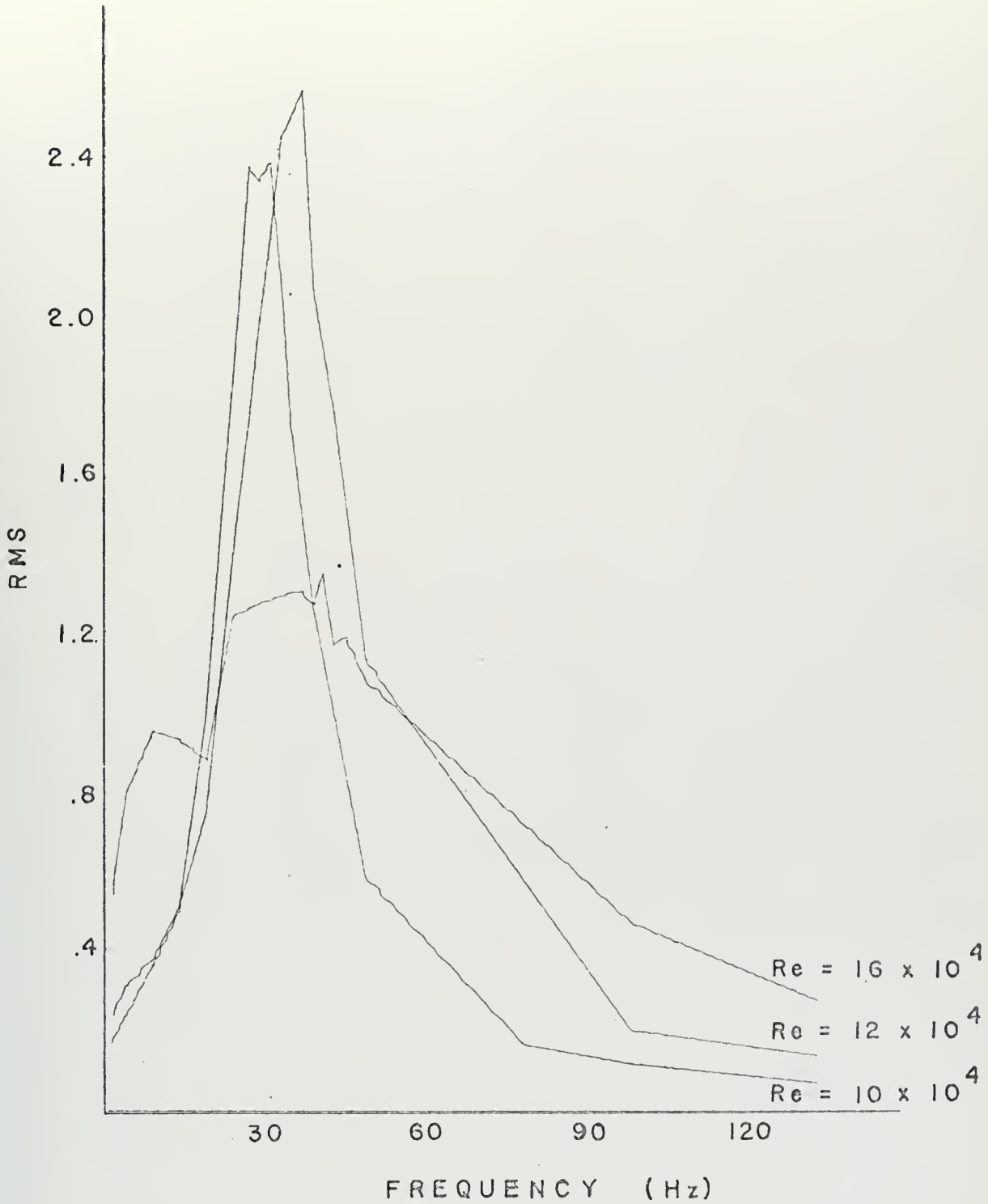

Figure 21: RMS VERSUS FREQUENCY
1 IN. DIAMETER ALUMINUM CYLINDER IN WATER

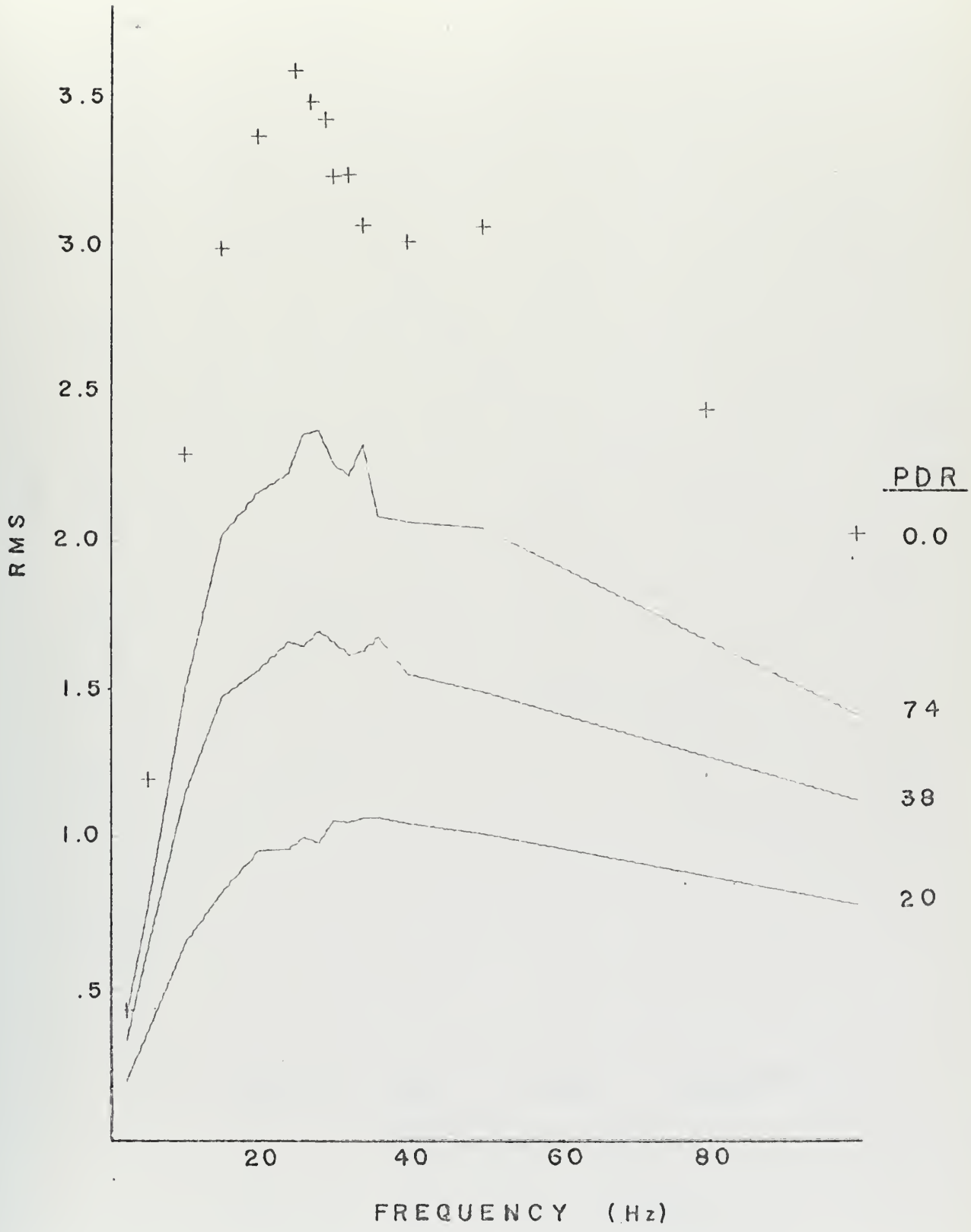

Figure 22: RMS VERSUS FREQUENCY
1 IN. PLEXIGLASS CYLINDER IN 25 WPPM SOLUTION
(Re = 10×10^4)

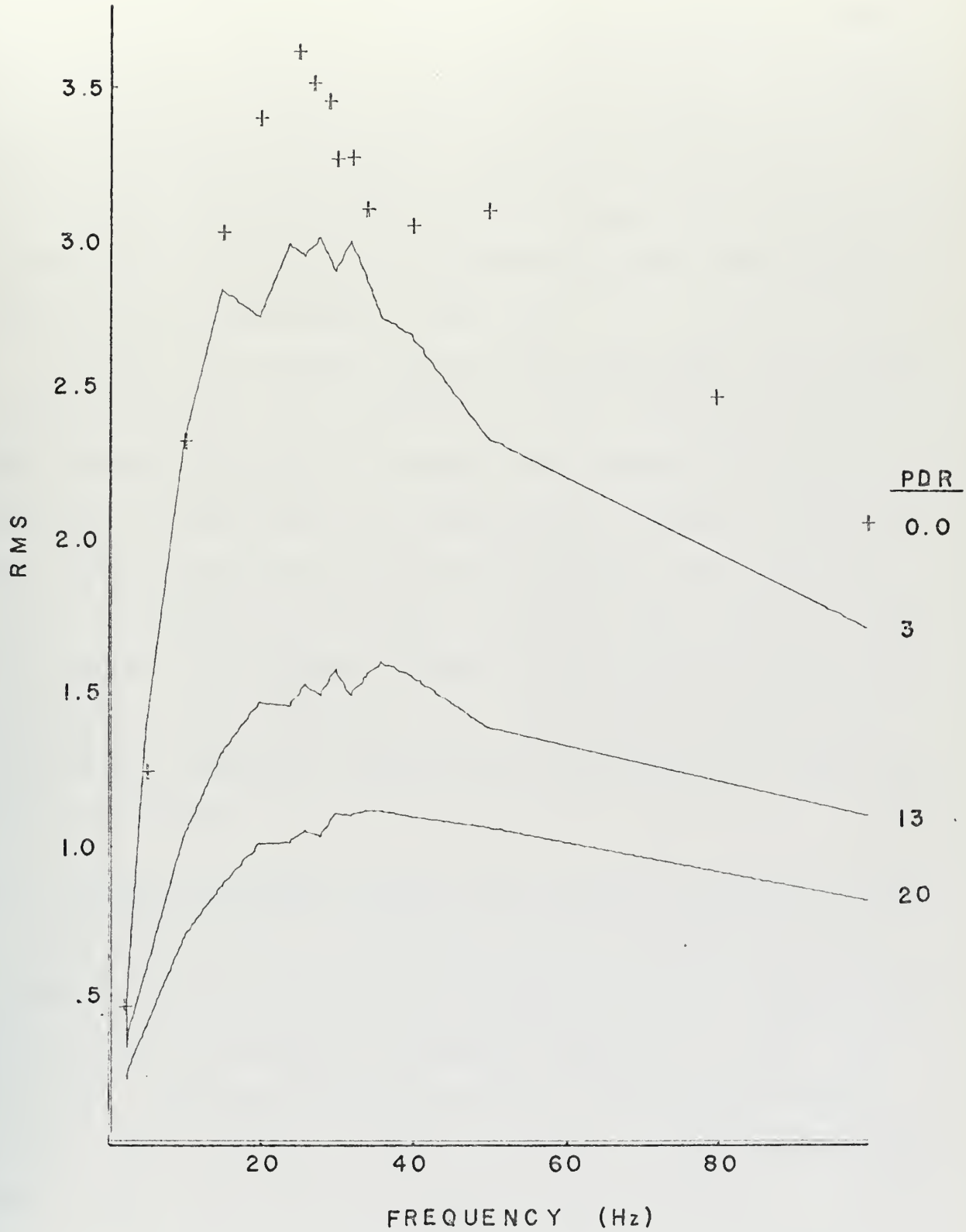

Figure 23: RMS VERSUS FREQUENCY
1 IN. PLEXIGLASS CYLINDER IN 25 WPPM SOLUTION
(Re = 10 x 10^4)

specific frequencies. The results of the two tests are presented in Figs. 24 and 25. The minimum value of RMS occurred in both tests at a PDR of 14%-20% for all frequencies but only three frequencies are graphed. The plot of the frequency at maximum RMS value versus PDR should indicate the nature of the predominant frequency as the spectrum changes. The plots for both tests are presented in Fig. 26.

One test was run with the one-inch plexiglass cylinder at a Reynolds number of 16×10^4 in 25 wppm polymer solution. The frequency spectrum at various PDR's showed a similar decrease in amplitude until a minimum was reached at 6.6% PDR. The solution remained at this point for over sever hours of running time and did not show a return to water behavior until the solution was diluted. Graphs of RMS versus Frequency are presented in Fig. 27 and Fig. 28. The plots of RMS versus PDR and the frequency of maximum RMS versus PDR are shown in Figs. 29 and 30.

D. FREQUENCY SPECTRUM AND DRAG FOR ONE-INCH ALUMINUM CYLINDER

Two tests were run with the aluminum cylinder to simultaneously monitor the drag and frequency spectrum measurements. The cylinder was tested at Reynolds numbers of 12×10^4 and 10×10^4. Frequency spectrum plots for the Reynolds number of 10×10^4 are shown in Figs. 31 and 32. Plots of RMS versus PDR for both tests are presented in Figs. 33 and 34.

The aluminum cylinder was also tested over a range of Reynolds numbers from 5×10^4 to 16×10^4 to determine the value

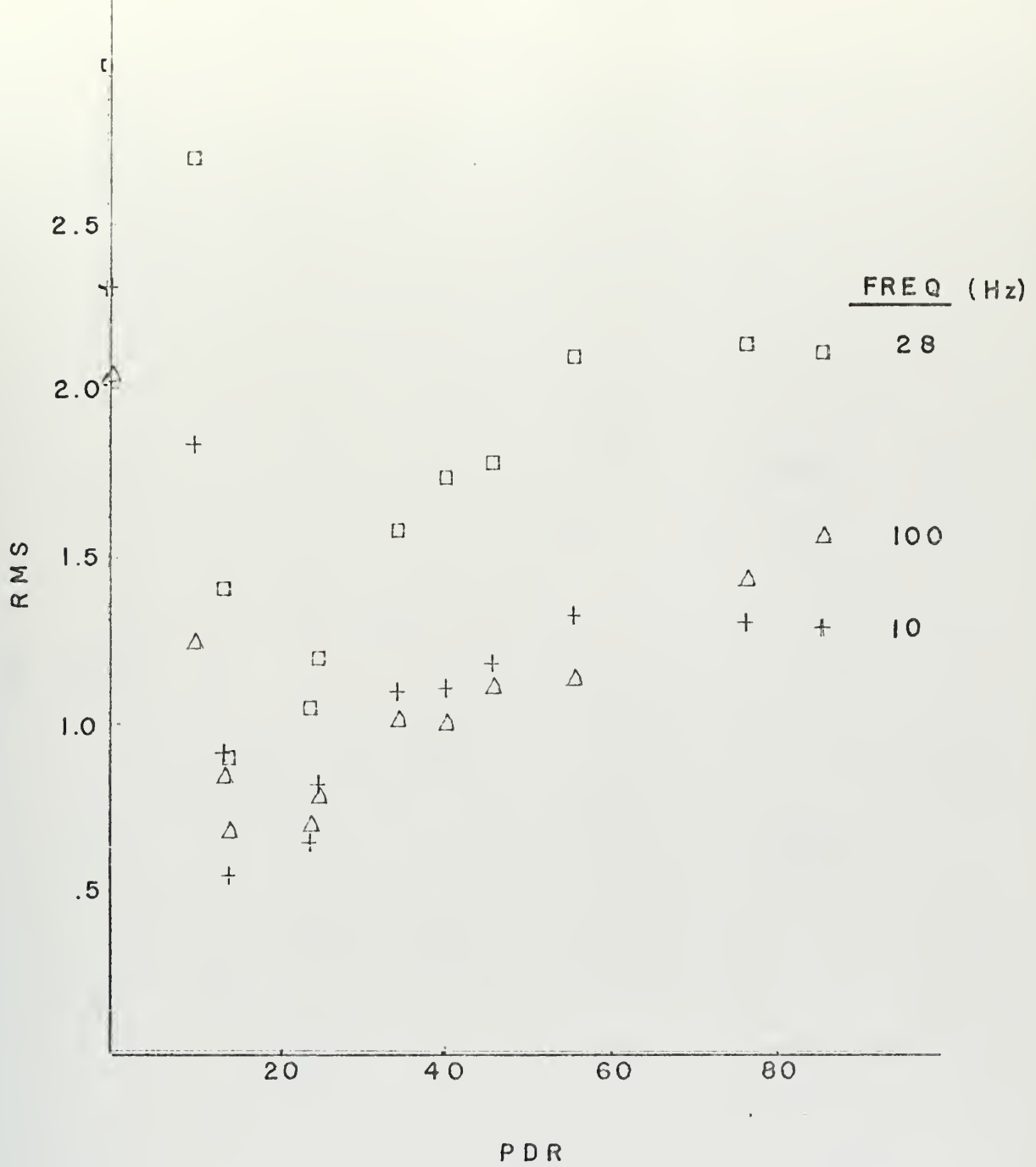

Figure 24: RMS VERSUS PDR
1 IN. PLEXIGLASS CYLINDER IN 25 WPPM SOLUTION
(Re = 10 x 10^4)

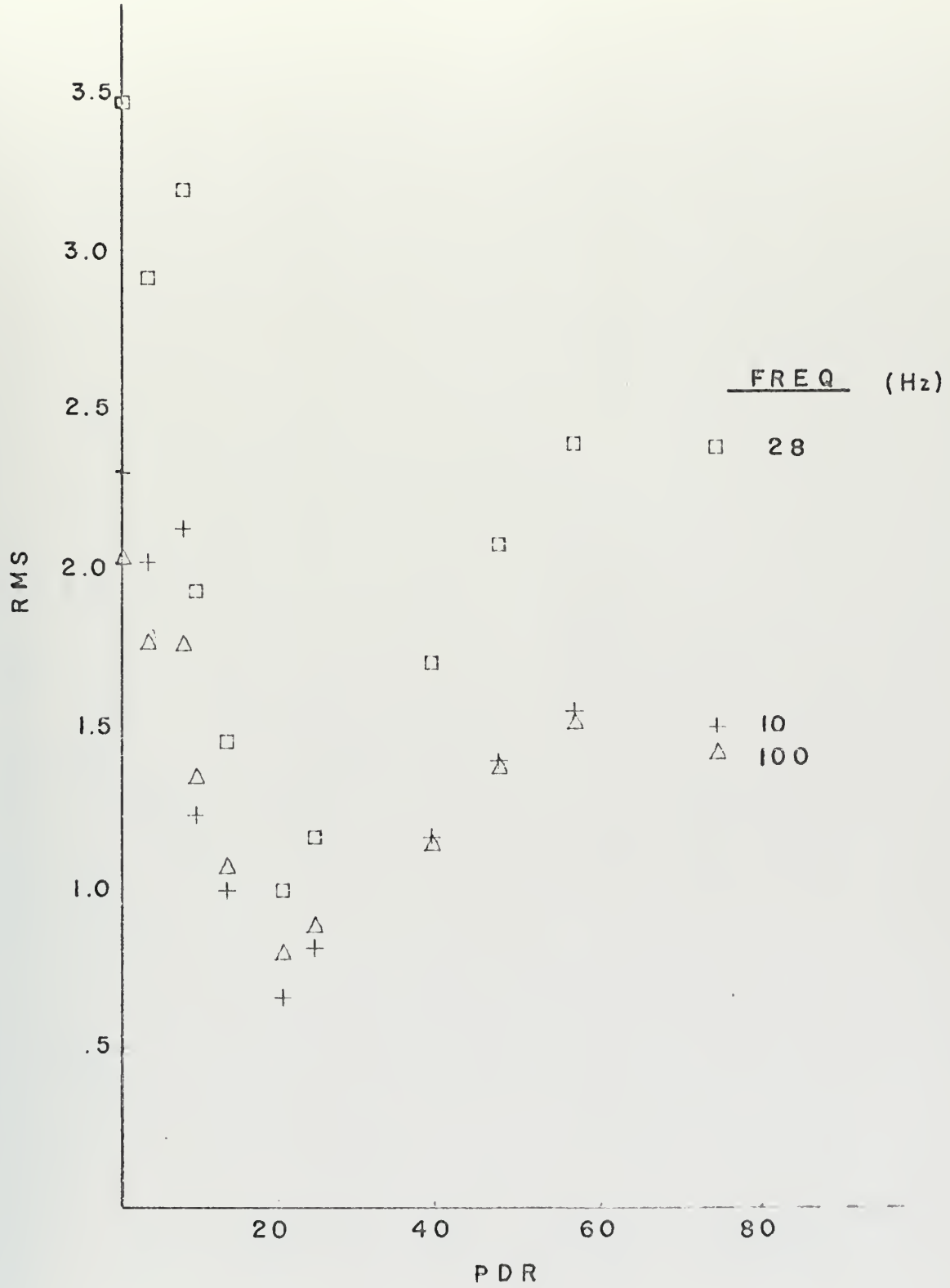

Figure 25: RMS VERSUS PDR
1 IN. PLEXIGLASS CYLINDER IN 25 WPPM SOLUTION
(Re = 10 x 10^4)

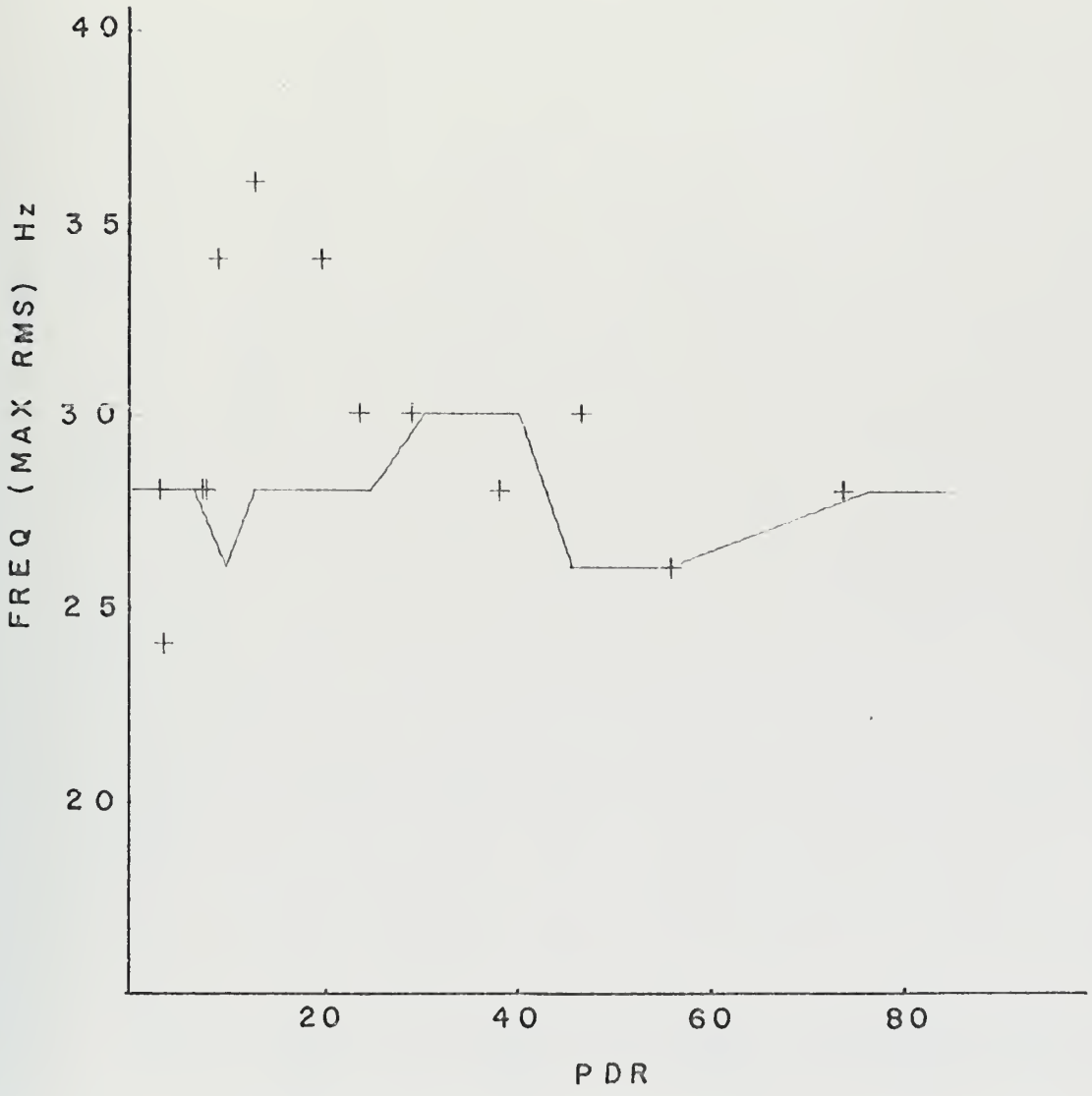

FIGURE 26: FREQUENCY (MAXIMUM RMS) VERSUS PDR
1 IN. PLEXIGLASS CYLINDER IN 25 WPPM SOLUTION
(Re 10 x 10^4)

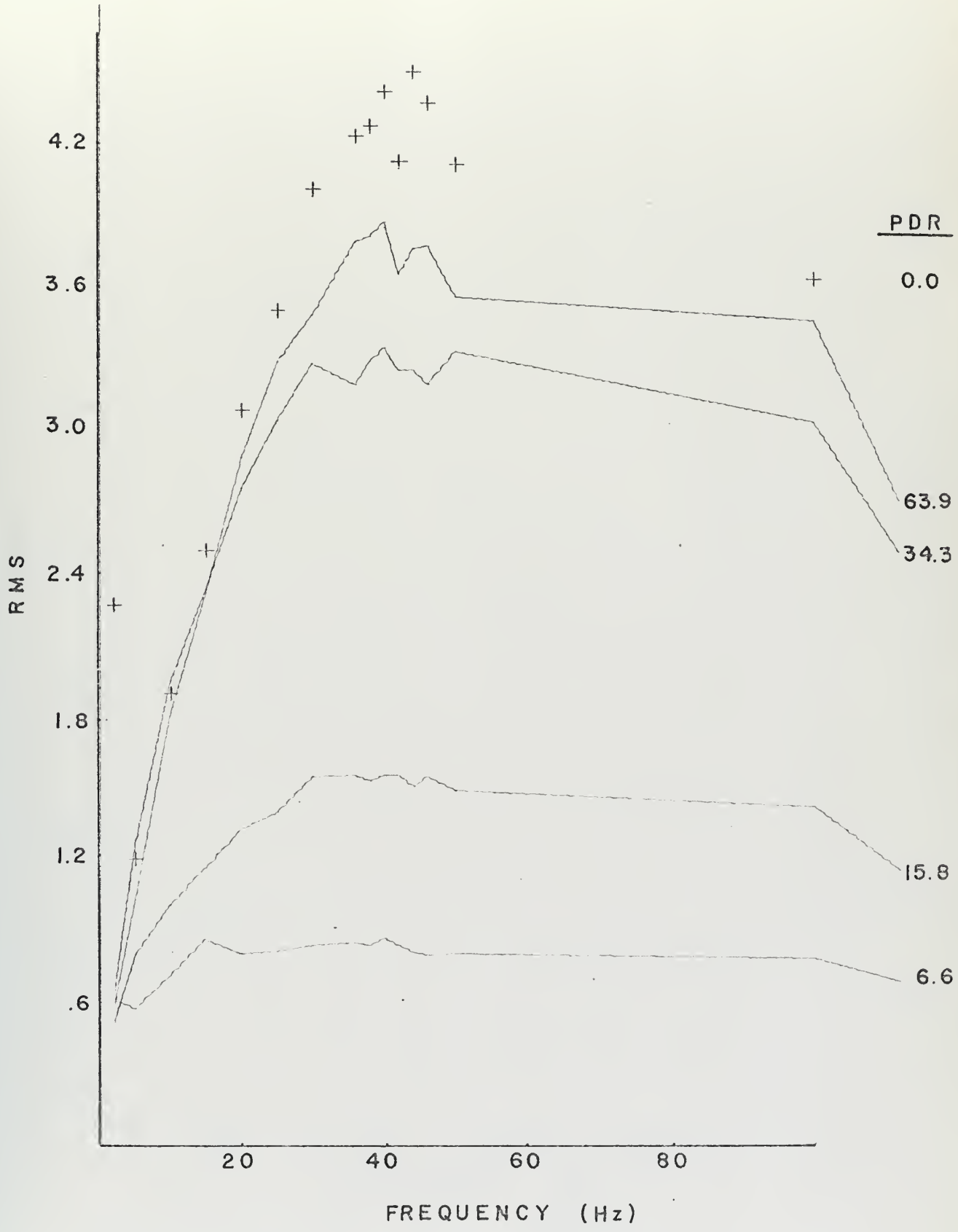

Figure 27: RMS VERSUS FREQUENCY
1 IN. PLEXIGLASS CYLINDER IN 25 WPPM SOLUTION
(Re = 10 x 10^4)

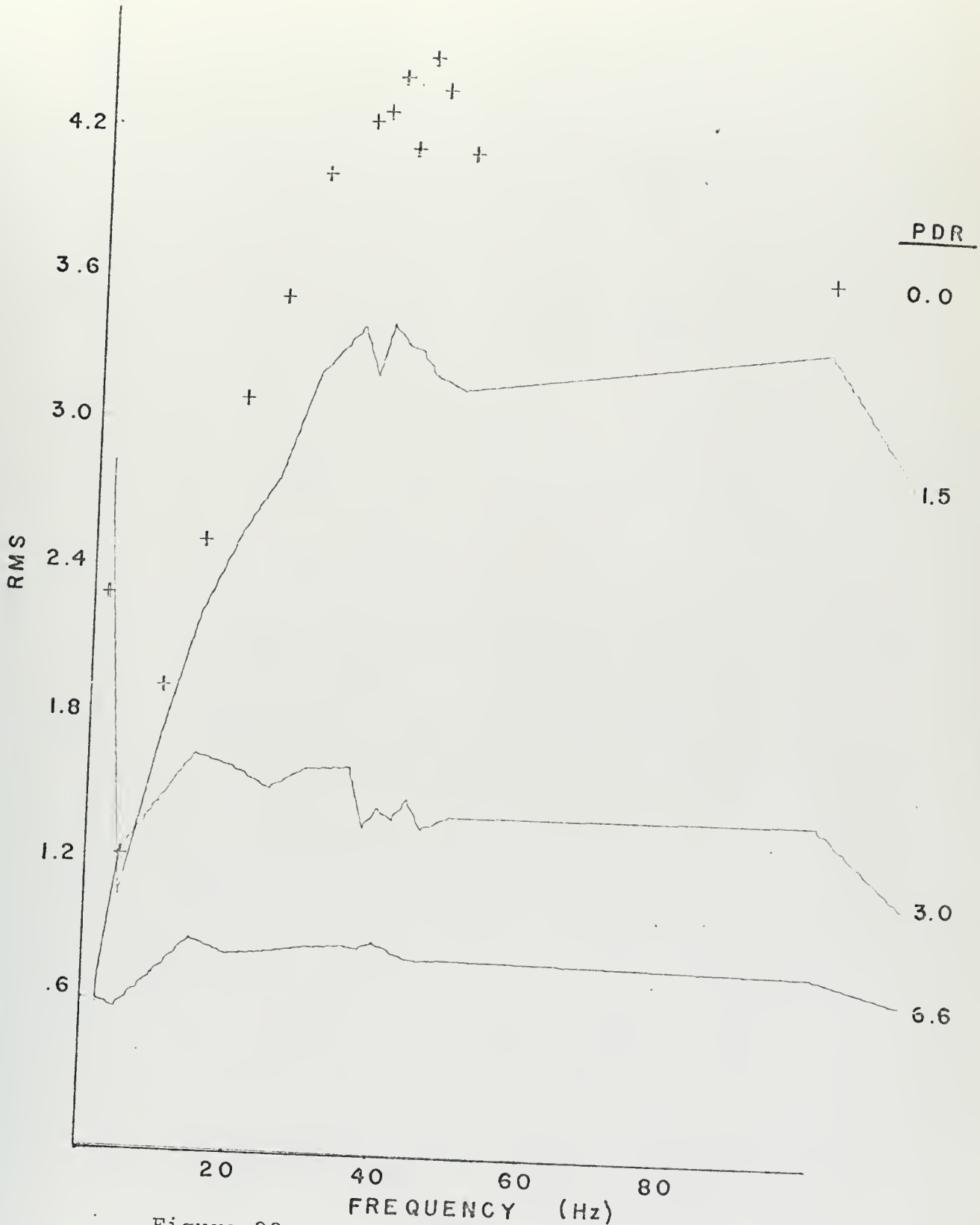

Figure 28: RMS VERSUS FREQUENCY
1 IN. PLEXIGLASS CYLINDER IN 25 WPPM SOLUTION
(Re = 10 x 10^4)

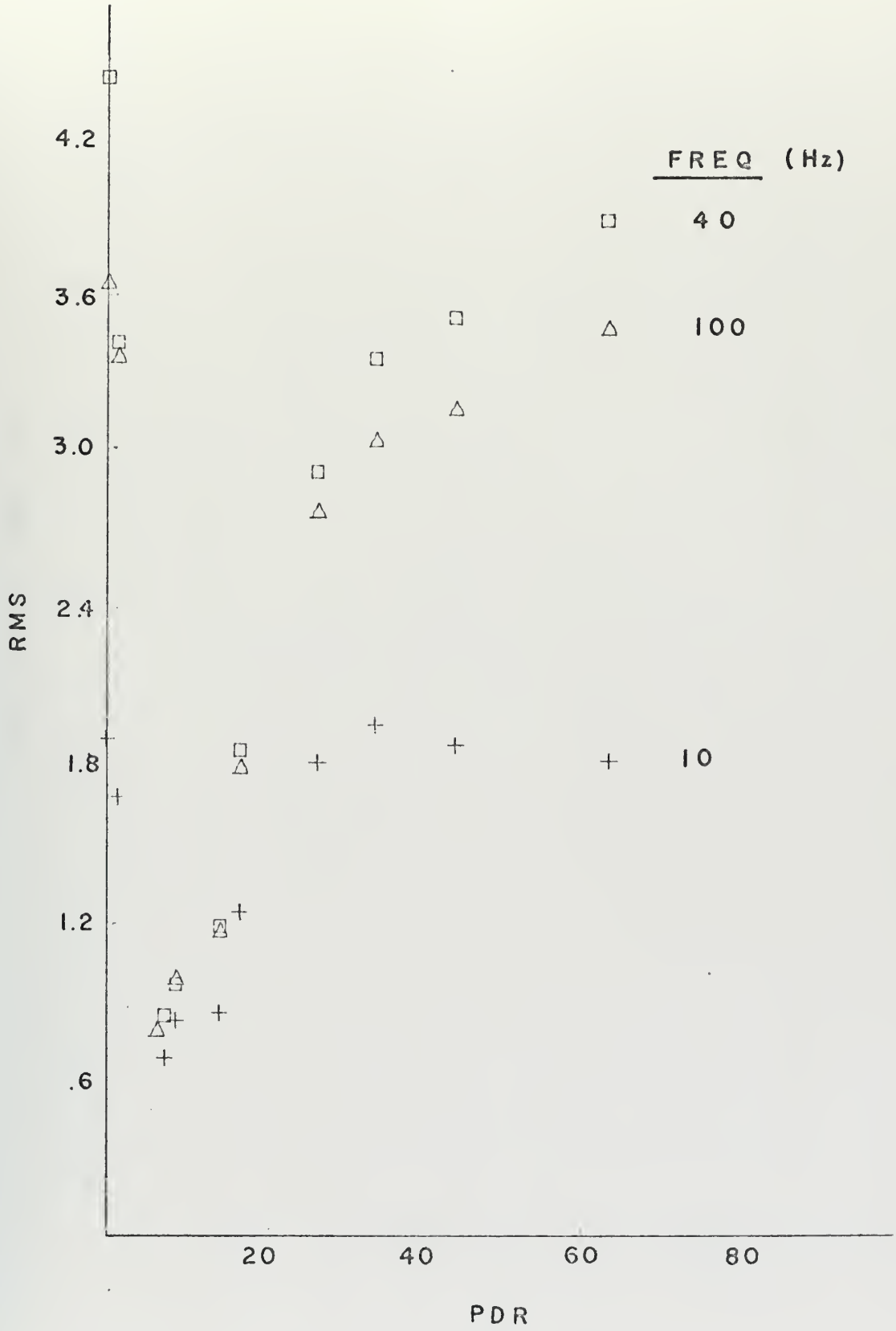

Figure 29: RMS VERSUS PDR
1 IN. PLEXIGLASS CYLINDER IN 25 WPPM SOLUTION
(Re = 16 x 10^4)

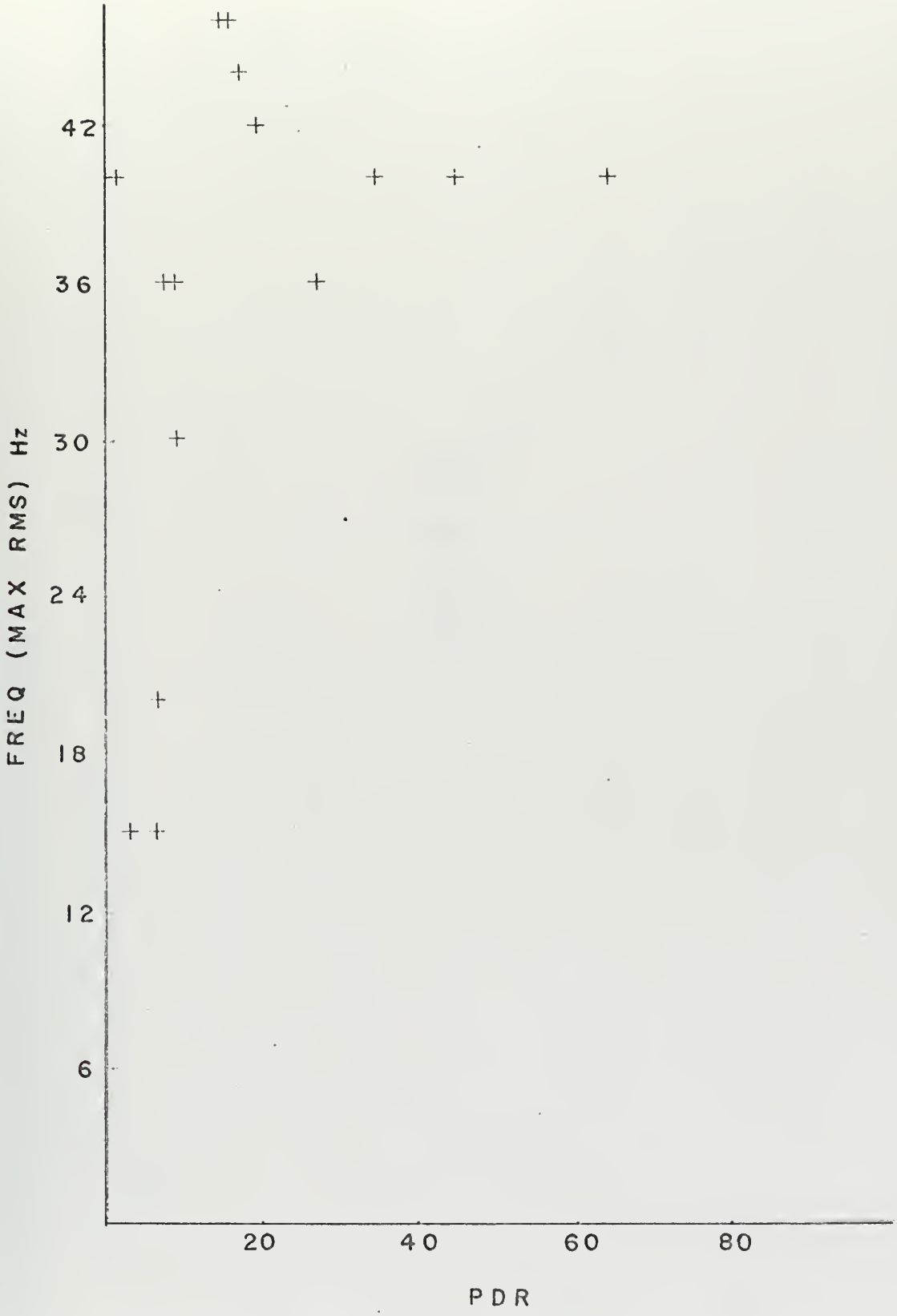

Figure 30: FREQUENCY (MAXIMUM RMS) VERSUS PDR
1 IN. PLEXIGLASS CYLINDER IN 25 WPPM SOLUTION
(Re = 16 x 10^4)

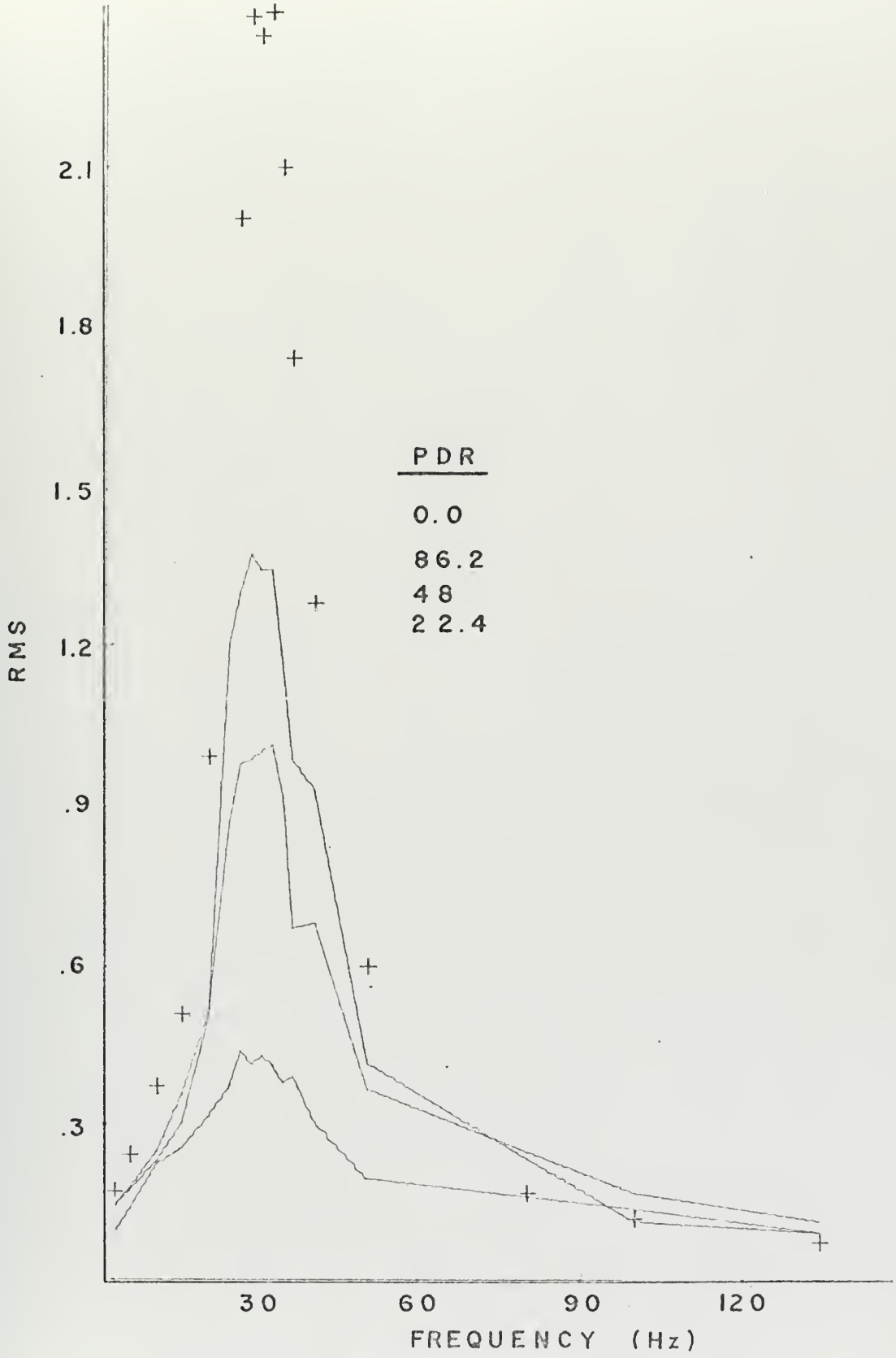

Figure 31: RMS VERSUS FREQUENCY
1 IN. ALUMINUM CYLINDER IN 25 WPPM SOLUTION
(Re = 10 x 10^4)

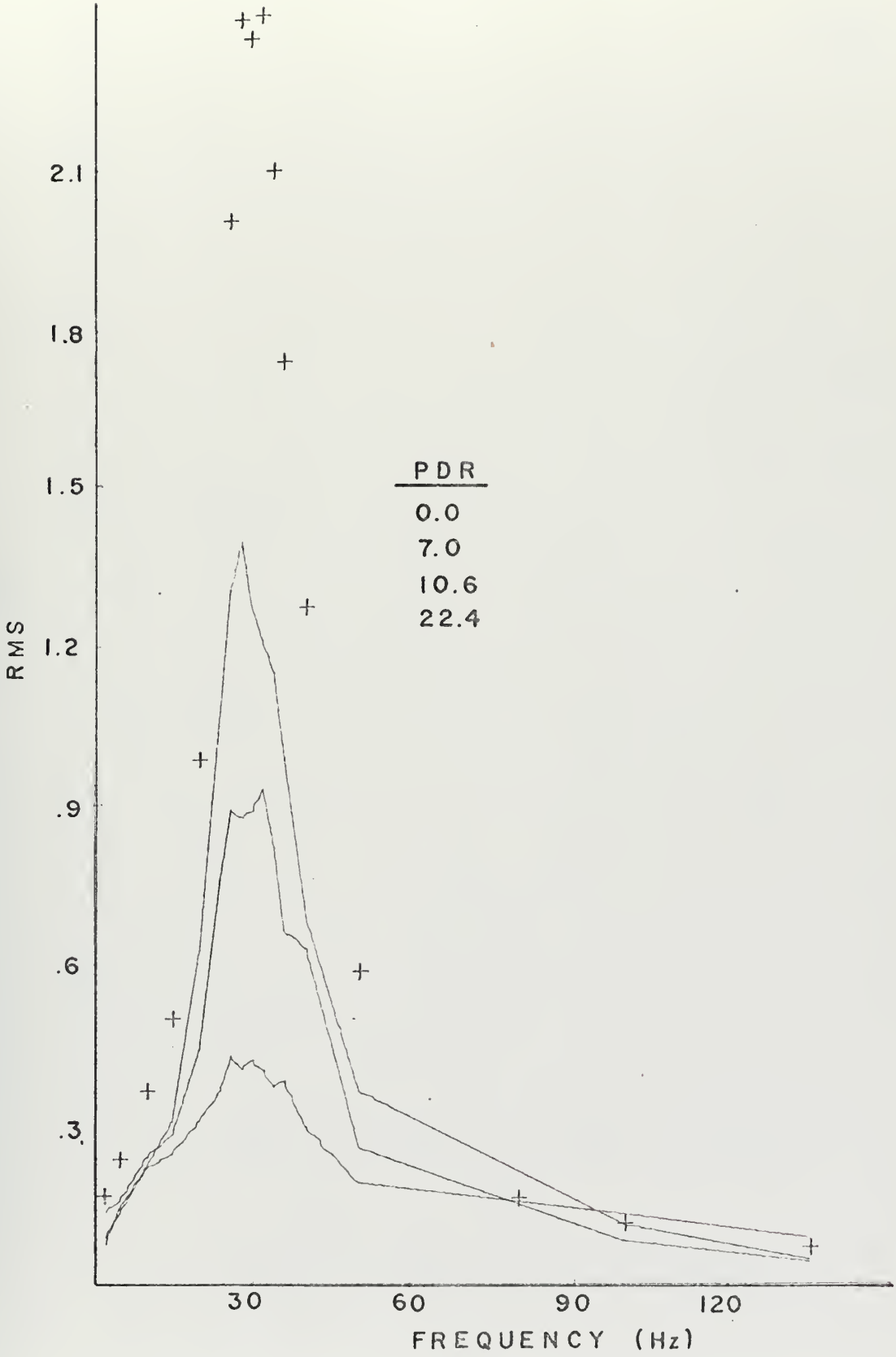

Figure 32: RMS VERSUS FREQUENCY
1 IN. ALUMINUM CYLINDER IN 25 WPPM SOLUTION
(Re = 10 x 10^4)

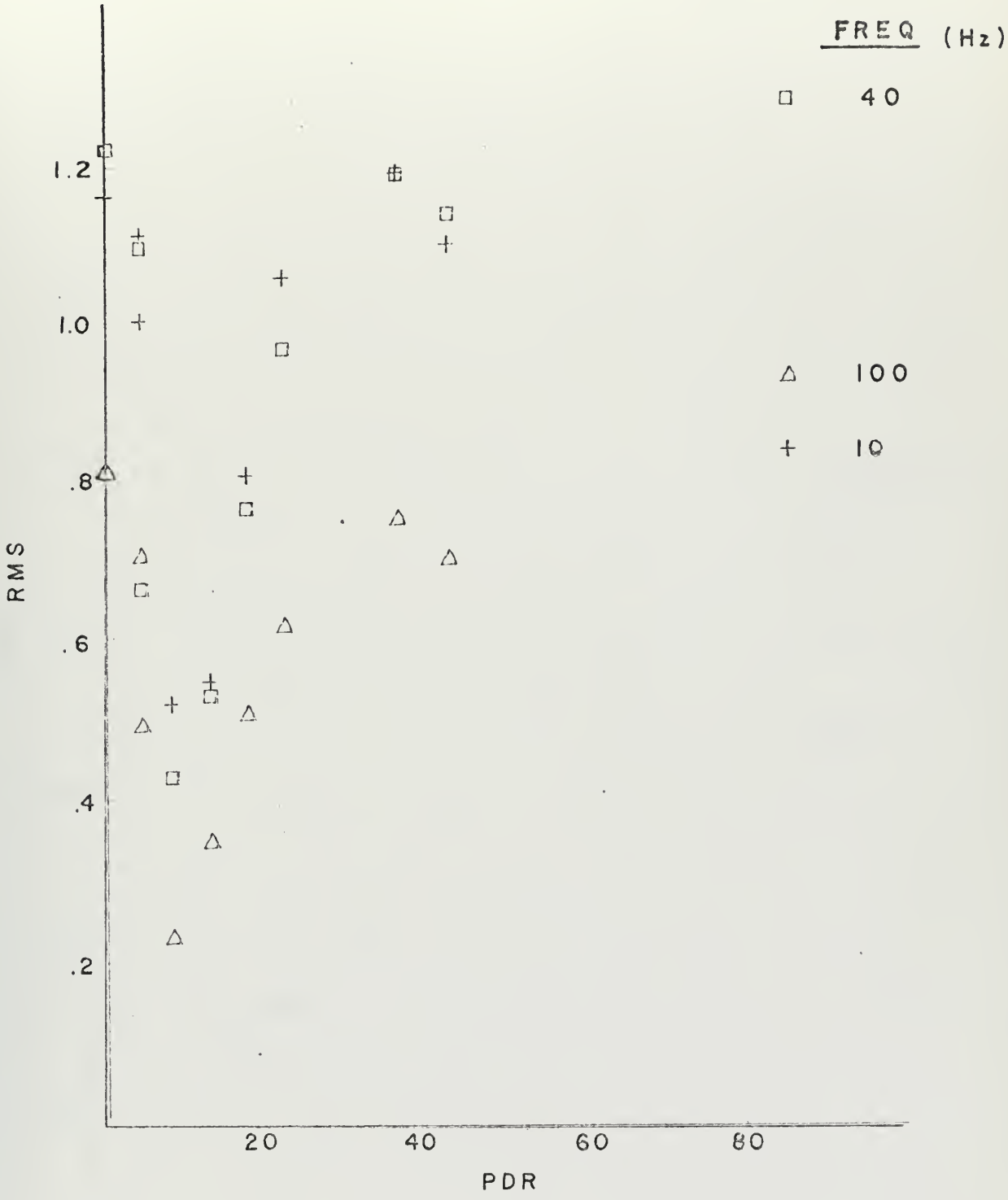

Figure 33: RMS VERSUS PDR
1 IN. ALUMINUM CYLINDER IN 25 WPPM SOLUTION
(Re = 12 x 10^4)

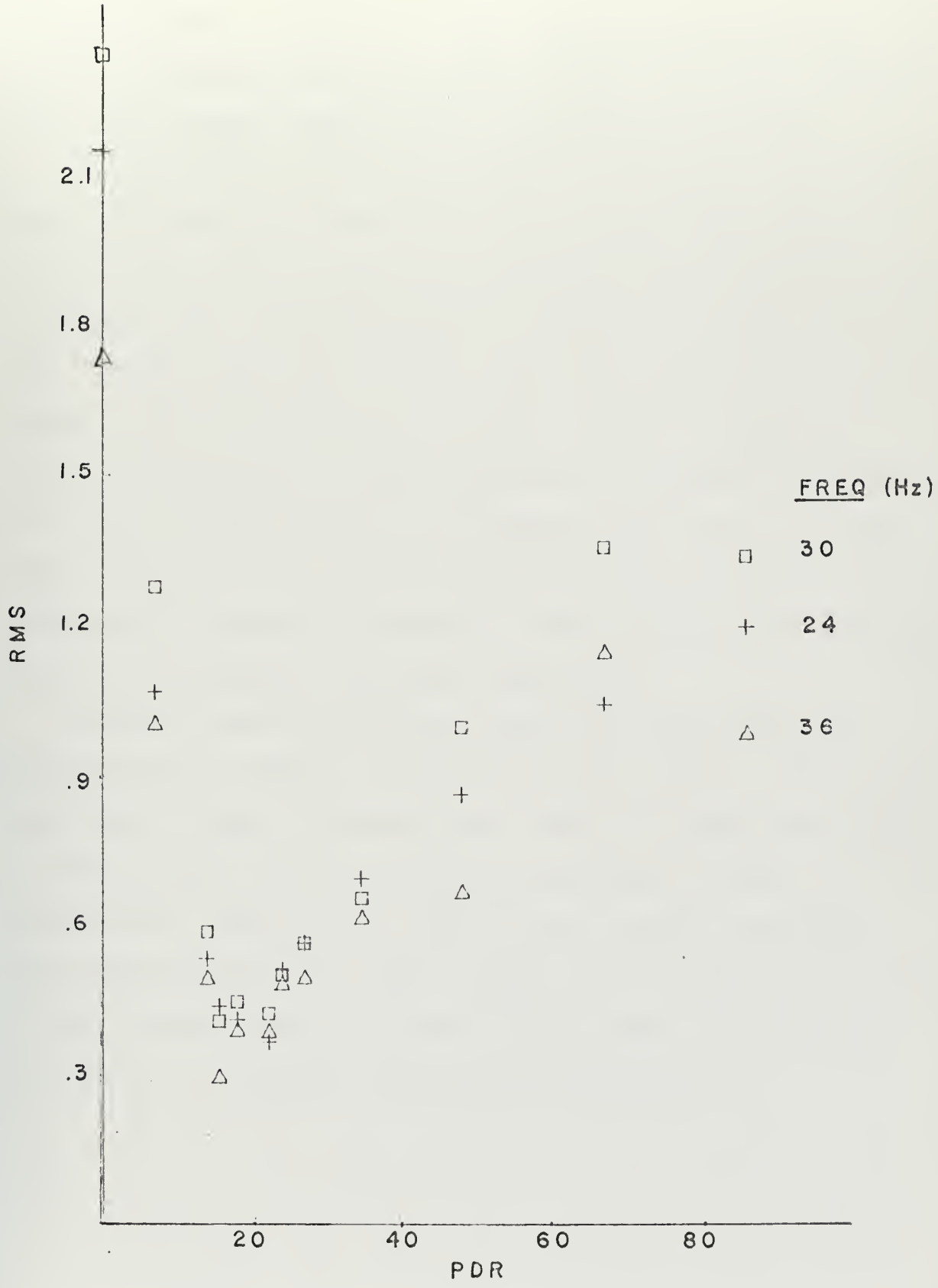

Figure 34: RMS VERSUS PDR
1 IN. ALUMINUM CYLINDER IN 25 WPPM SOLUTION
(Re = 10 x 10^4)

of C_d in water. (Fig. 35). This plot has shown that the cylinder enter the critical region at Re = 13 x 10^4, agreeing with the Strouhal frequency data previously presented.

To facilitate the correlation of the frequency and drag data, two plots were made on the same graph. The top plot shows maximum value of RMS versus PDR while the lower one shows C_d versus PDR. (Figs. 36 and 37). There is a direct correlation between the maximum value of RMS and the Strouhal frequency: When the RMS value is high or close to the water value, a predominant Strouhal frequency is present; and when it is at a minimum, there is no dominant frequency. In both cases the drag crisis occurs simultaneously with the re-establishment of a dominant frequency. This fact can be seen in the graphs of maximum RMS frequency versus PDR.

Frequency spectrum analyses were also made on the drag signals before, during, and after the drag crisis. These plots are shown in Figs. 38 through 40. The major point observed in these graphs is the increased predominance of the low frequencies. After crisis, when C_d and Strouhal frequency have returned to a water-like value, a very strong low frequency is still predominant in the oscillating drag. Chart records of drag and pressure are prescribed in Appendix C.

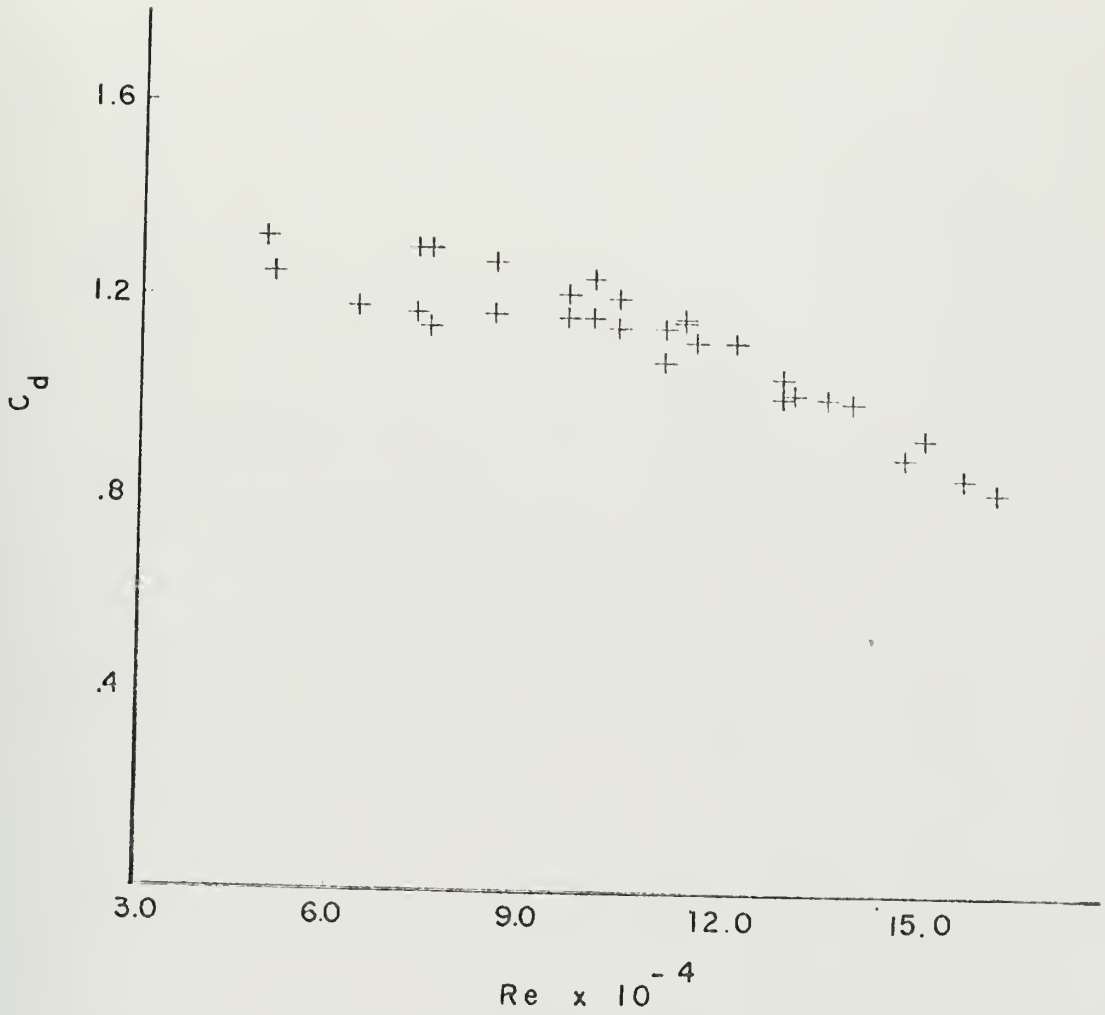

Figure 35: C_d VERSUS Re
1 IN. DIAMETER ALUMINUM CYLINDER IN WATER

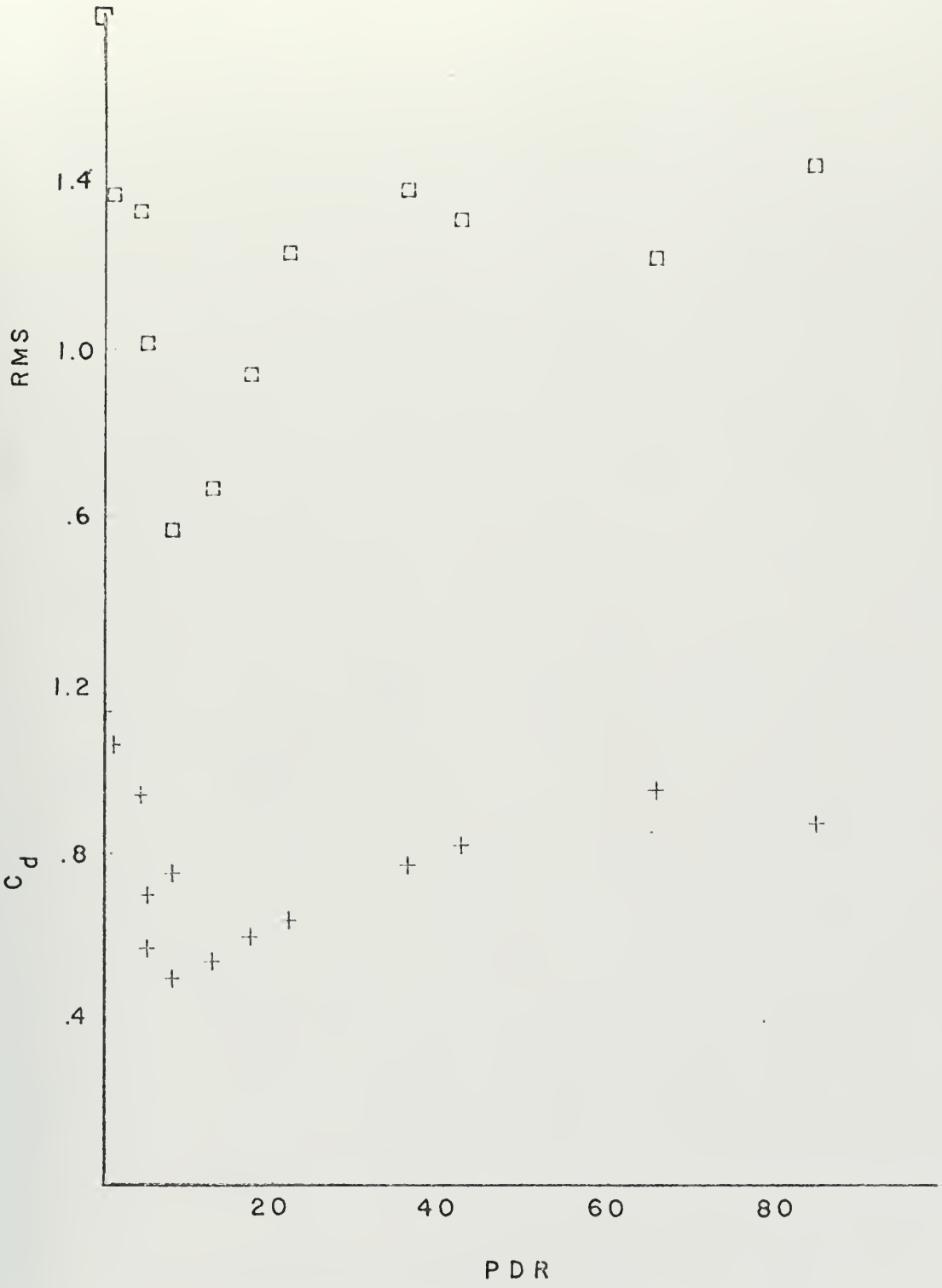

Figure 36: MAXIMUM RMS, C_d VERSUS PDR
1 IN. ALUMINUM CYLINDER IN 25 WPPM SOLUTION
(Re = 12 x 10^4)

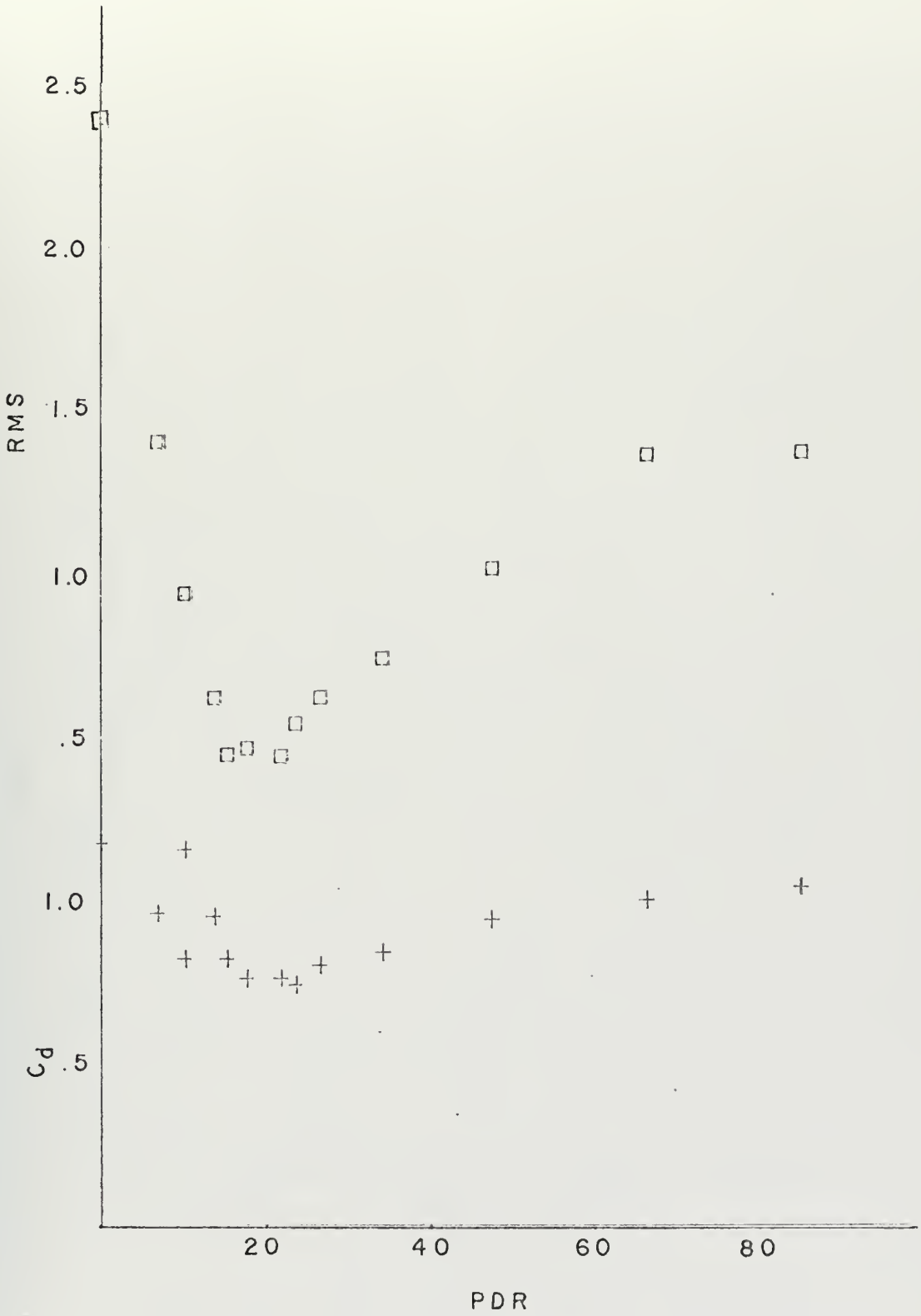

Figure 37: MAXIMUM RMS, C_d VERSUS PDR
1 IN. ALUMINUM CYLINDER IN 25 WPPM SOLUTION
(Re = 10 x 10^4)

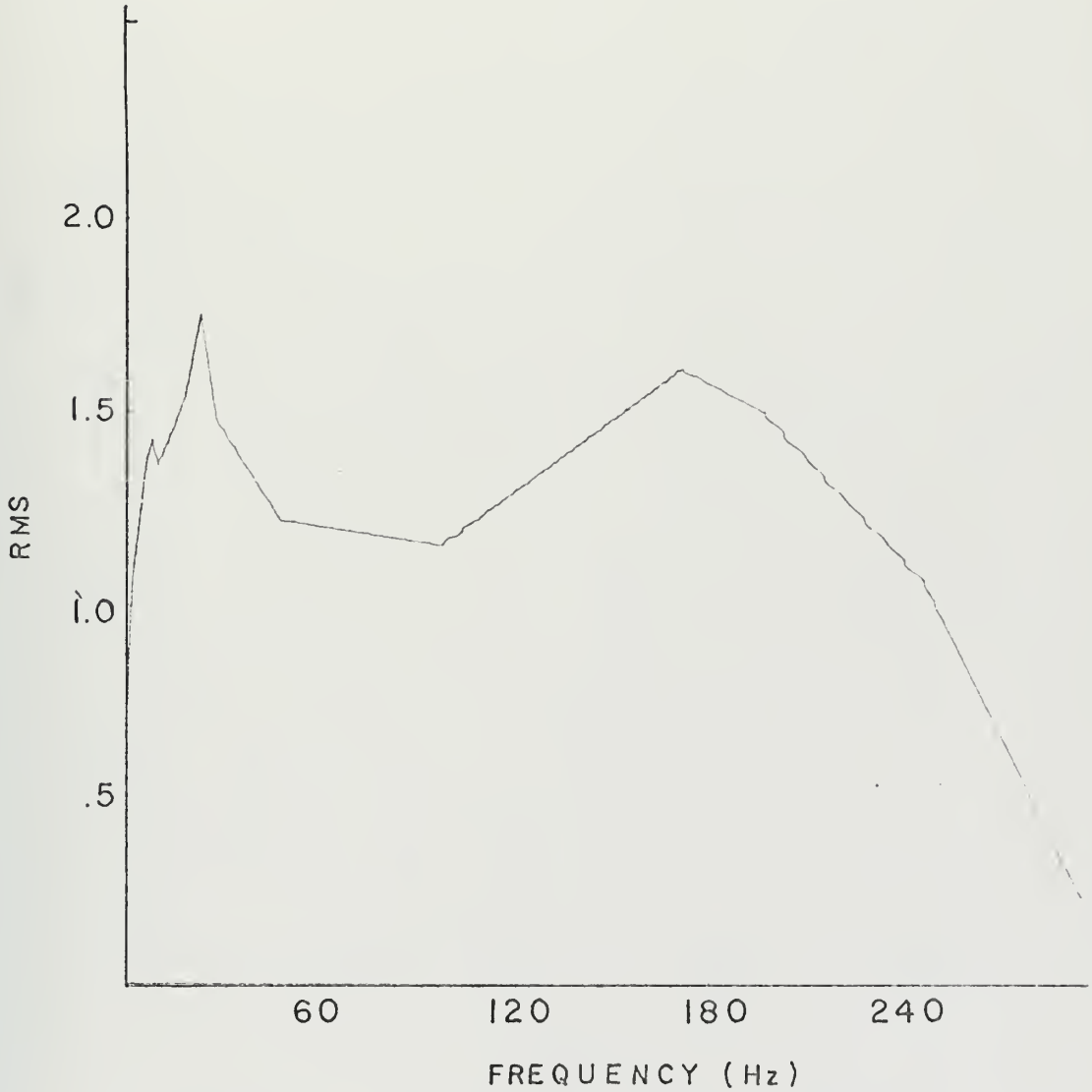

Figure 38: RMS (DRAG) VERSUS FREQUENCY
1 IN. ALUMINUM CYLINDER IN 25 WPPM SOLUTION
(Re = 10 x 10^4) BEFORE CRISIS

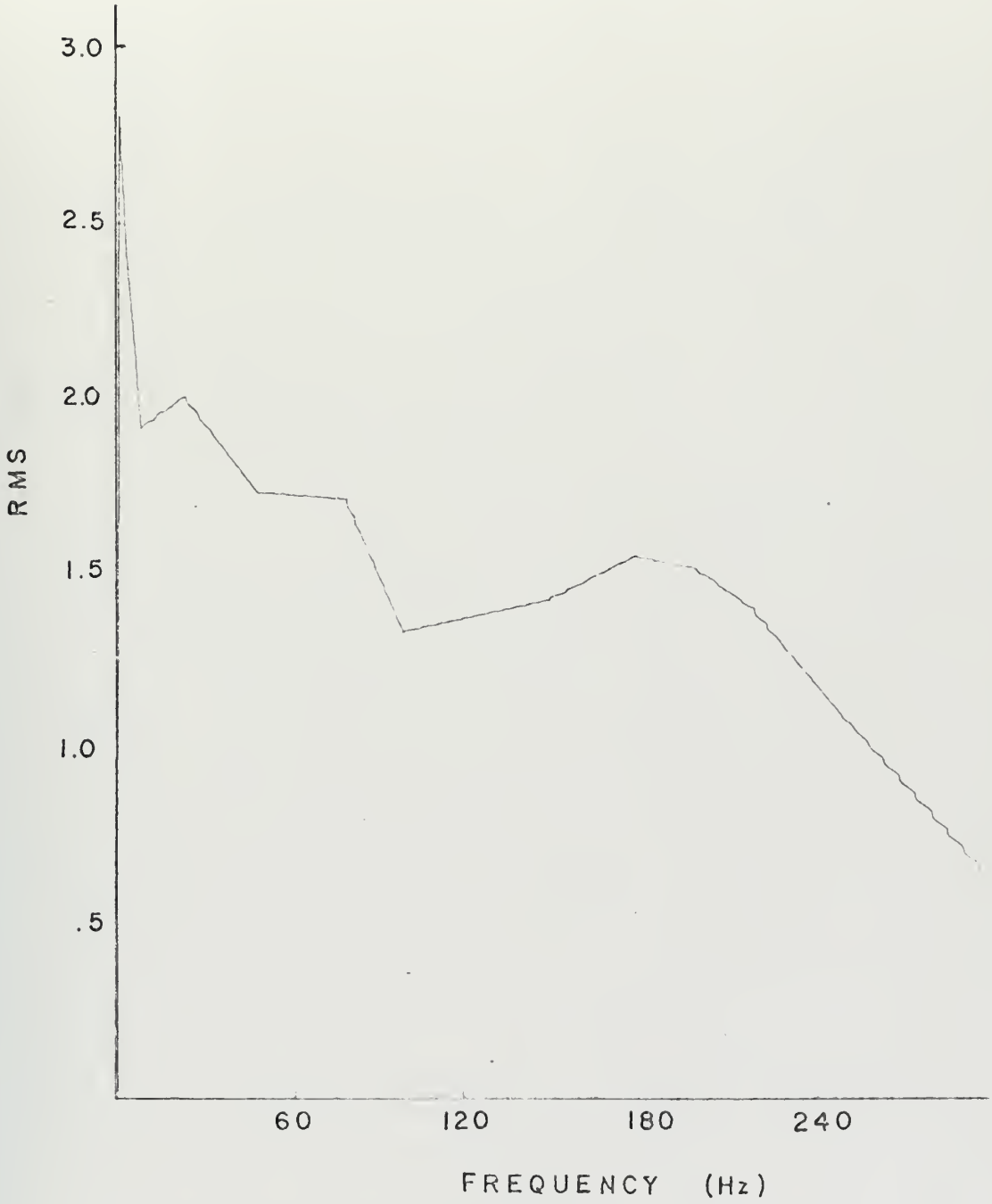

Figure 39: RMS (DRAG) VERSUS FREQUENCY
1 IN. ALUMINUM CYLINDER IN 25 WPPM SOLUTION
(Re = 10 x 10^4) DURING CRISIS

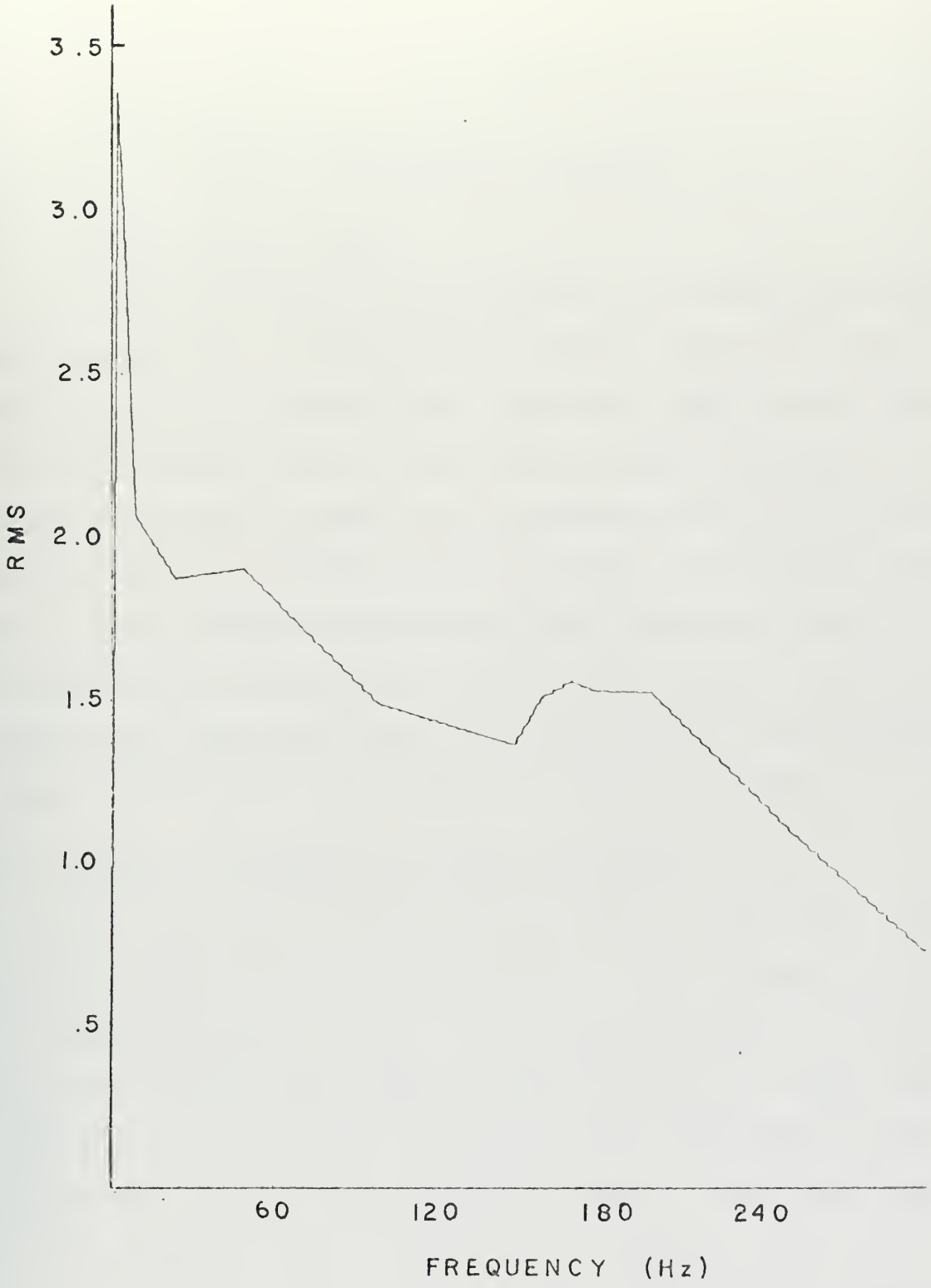

Figure 40: RMS (DRAG) VERSUS FREQUENCY
1 IN. ALUMINUM CYLINDER IN 25 WPPM SOLUTION
(Re = 10×10^4) AFTER CRISIS

IV. DISCUSSION OF RESULTS

A. STROUHAL NUMBER DATA

The data presented in this section have shown the accuracy and repeatability of the pressure sensing equipment. The plots of Strouhal number versus Reynolds number agreed with previous results found in the fluid dynamics literature. Graphs of Strouhal numbers were extremely useful in the prediction of the transition Reynolds number. The early transition on the one-inch aluminum cylinder indicated that the boundary layer stability is strongly dependent on the end conditions. This dependence could be caused by three-dimensional effects or by the vibration of the cylinder.

B. FREQUENCY SPECTRUM IN POLYMER SOLUTIONS

The frequency spectrum plots agreed very well with Strouhal frequency data indicating the accuracy and repeatability of the bandpass filter method. No noticeable change in frequency was noted between water and dilute polymer at the same Reynolds number. The change was a decrease in the amplitude of the polymer RMS signal when compared to water. The polymer appears to have caused a shift in the vortex formation point or increased the circulation of the vortex thus causing a lower RMS signal. As the polymer degrades, the molecular weight changes until a point is reached where concentration, Reynolds number, and body-diameter combination becomes such that the

transition occurs in the boundary layer. In fresh solutions, the polymer molecules entangle in a continuum that dissipates energy in the polymer molecules and causes a shift in separation of increase in circulation. In a highly stable low Reynolds number region, this energy dissipation increases the frequency of shedding as noted by Gadd and others.

C. FREQUENCY AND DRAG COMBINED

The similarity of the curves of maximum RMS and C_d versus PDR can be comined into a single general curve depicting the various flow regimes as affected by PDR (Fig. 41). Initially for PDR > 60, the polymer solution behaves like water in a subcritical regime with only small changes in C_d, C_p, oscillating lift, pressure signatures, and Strouhal frequency. [Refs. 19, 24, 27]. As degradation occurs (a decrease in molecular weight) the flow enters the transition region with C_d, C_p and Strouhal number effected in a similar manner as in transition in water. When the PDR had decreased to a certain value, the degraded polymer begins to lose its effectiveness and the boundary layer begins to shift from turbulent to laminar regime. The magnitude of the oscillations suggest that this is a circumferential rather than a longitudinal shift.

The addition of polymer to water causes water-like effects to occur at lower Reynolds numbers dependent on the concentration. At one Reynolds number several regimes of flow can be observed as the polymer degrades.

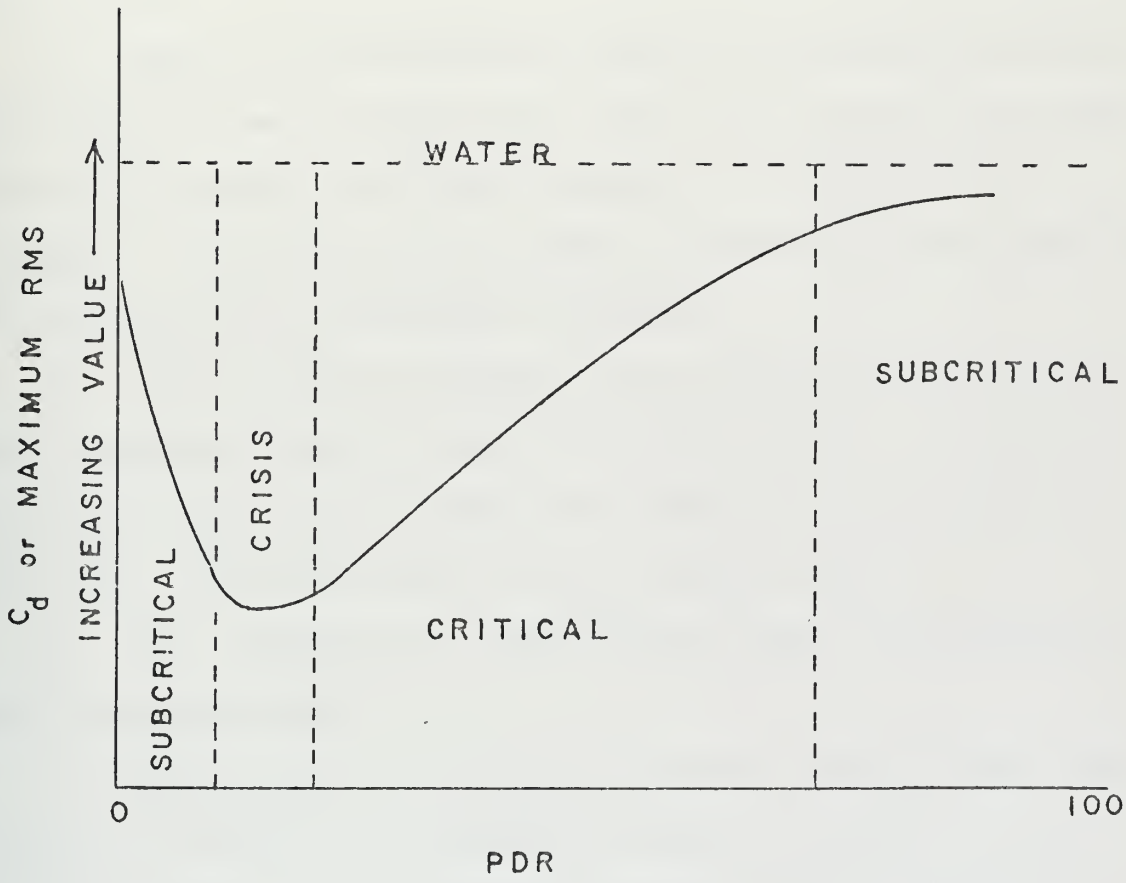

Figure 41: COMPARISON OF C_d AND MAXIMUM RMS WITH REGIMES OF FLOW

V. CONCLUSIONS

The data presented herein warrant the following conclusions:

1. There is no noticeable change in the vortex shedding frequency at the same Reynolds number of a circular cylinder immersed in water from that immersed in a dilute polymer solution. In fact the only change is degrees in the amplitude of the RMS signal in polymer solutions.

2. As the polymer degrades, the molecular weight gradually decreases until a state is reached where concentration, Reynolds number and the body-size combination becomes such that the transition occurs in the boundary layer.

3. The transition is amplified by large oscillations in the drag coefficient.

4. The addition of polymer to water causes water-like effects to occur at low Reynolds numbers dependent on the concentration. At one Reynolds number several regions of flow may be observed as the polymer degrades.

VI. SUGGESTIONS FOR FUTURE WORK

It is recommended that:

1. The variation of the intensity of turbulence as a function of the degration of polymer be determined with a hot film probe;

2. The vortex shedding frequency be re-evaluated by placing a hot film probe at a suitable location downstream of the cylinder; and finally

3. Experiments be carried out on axisymmetric bodies with semi-spherical or other head forms.

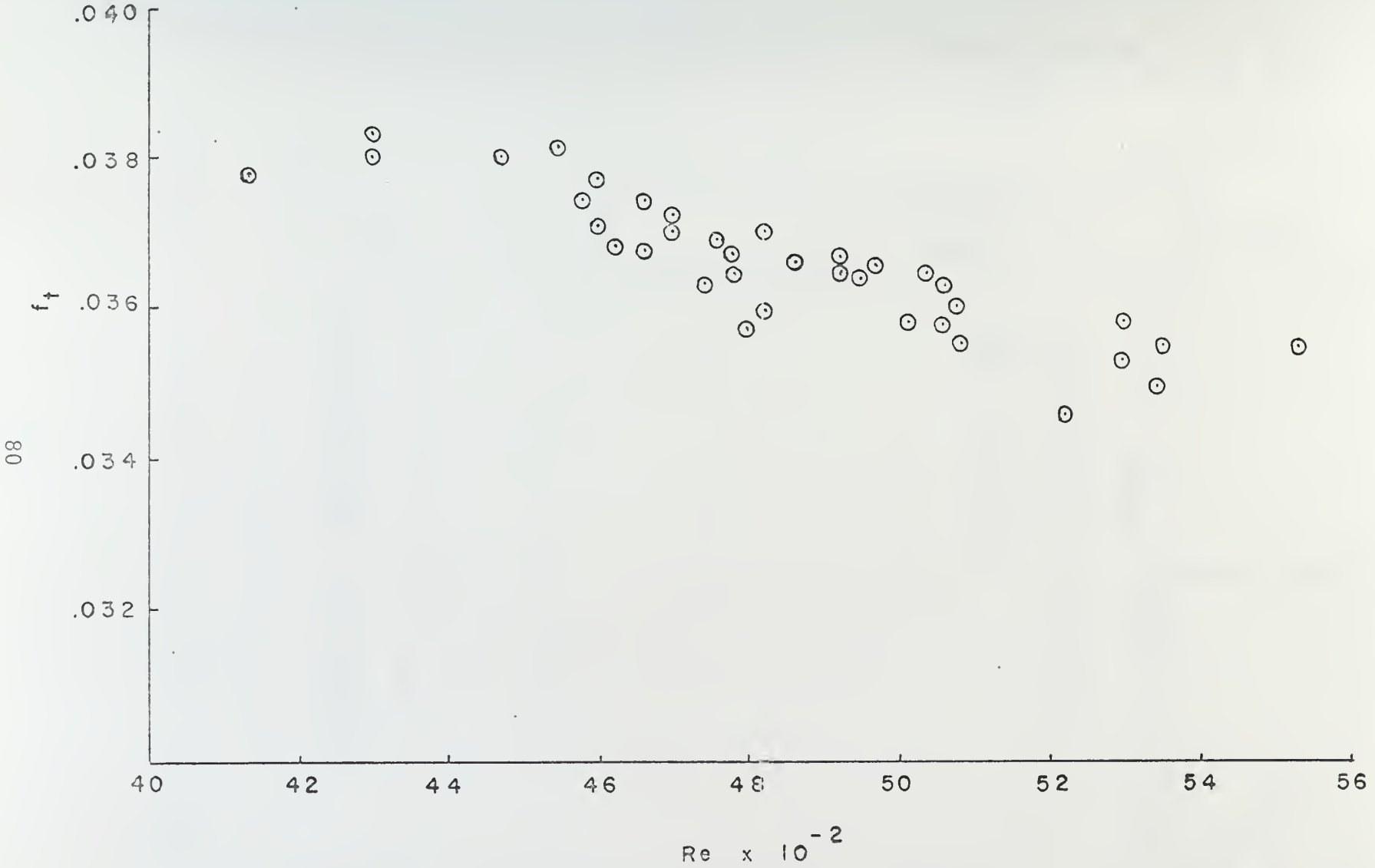

APPENDIX A: FANNING FRICTION FACTOR FOR TAP WATER

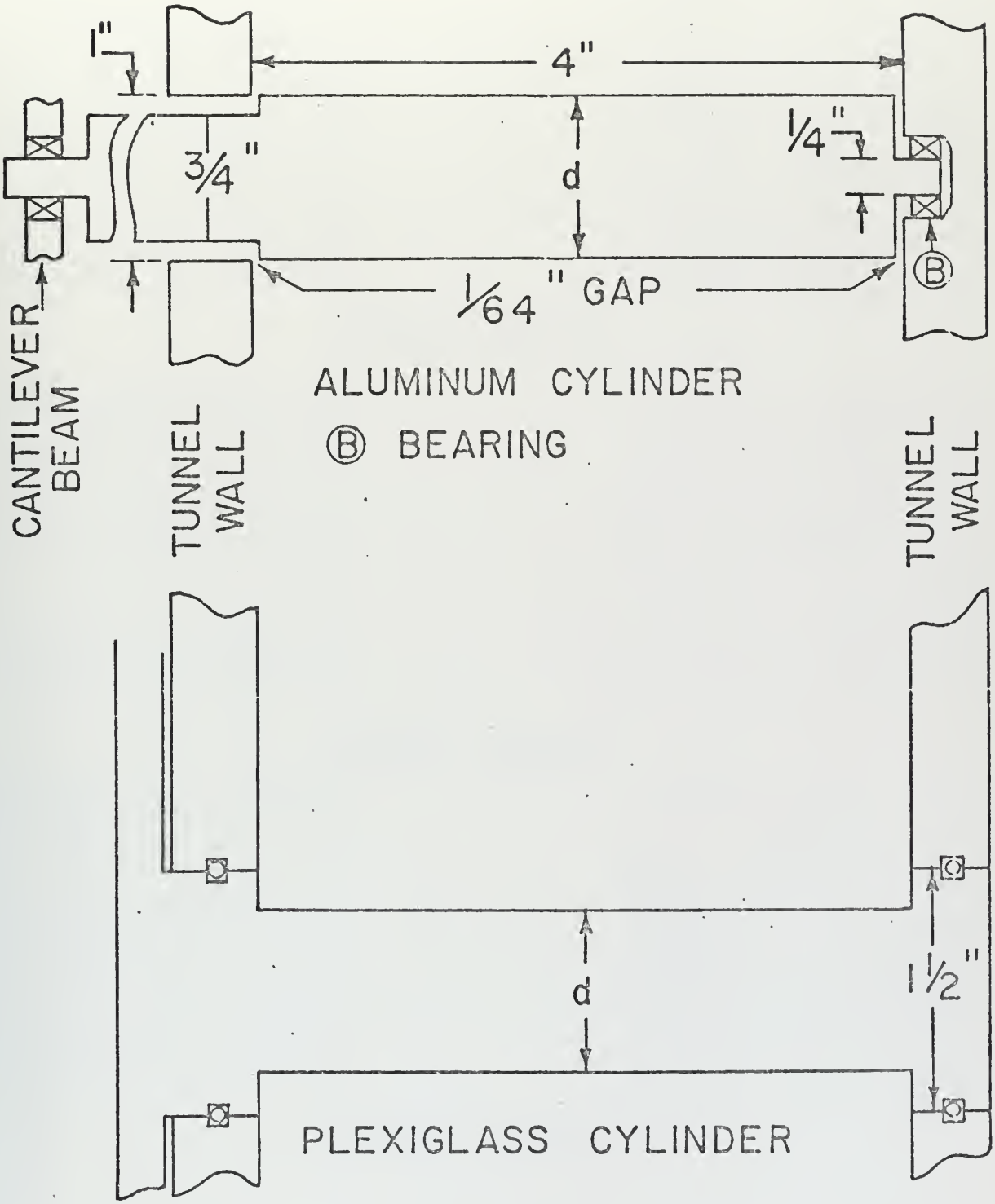

APPENDIX B: COMPARISON OF CYLINDER END CONDITIONS

PRESSURE

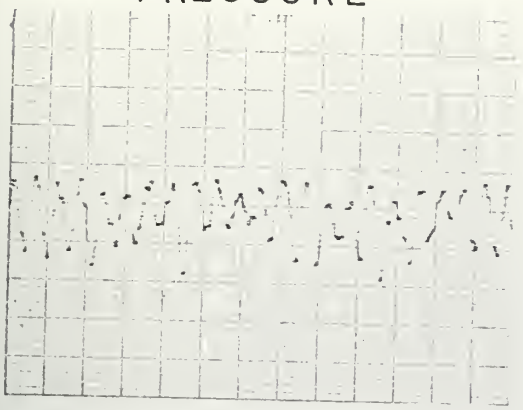

DRAG

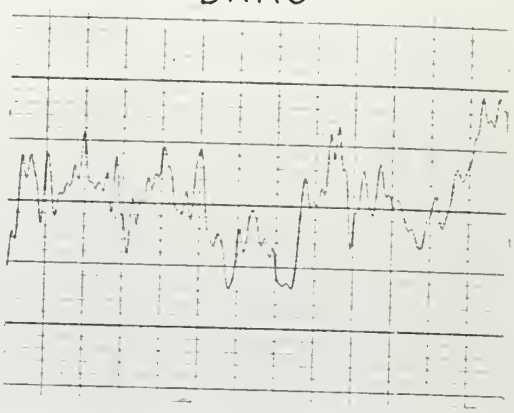

BEFORE CRISIS

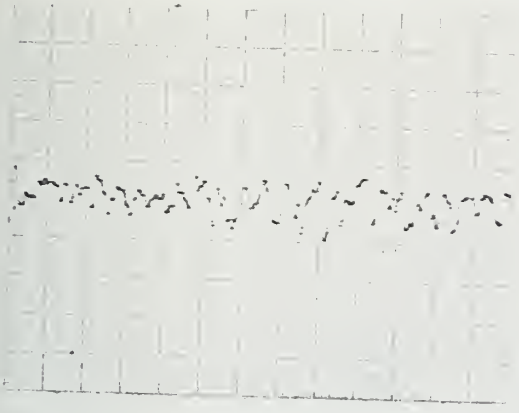

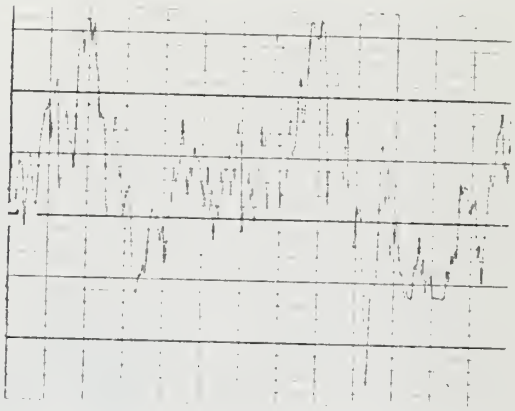

DURING CRISIS

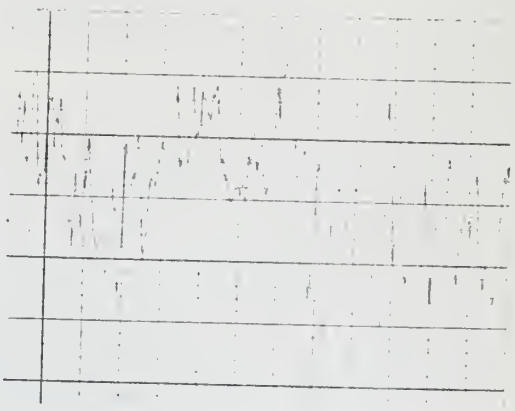

AFTER CRISIS

APPENDIX C: DRAG AND PRESSURE CHART RECORDS

DRAG SIGNALS (25 wppm)

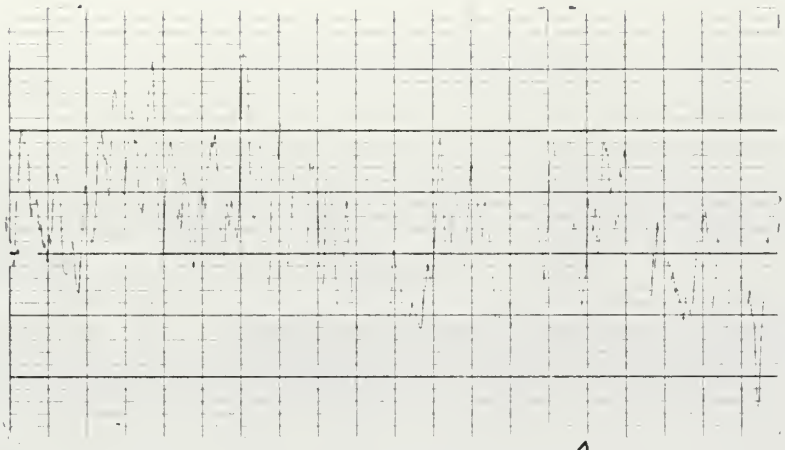

$Re = 7.5 \times 10^4$

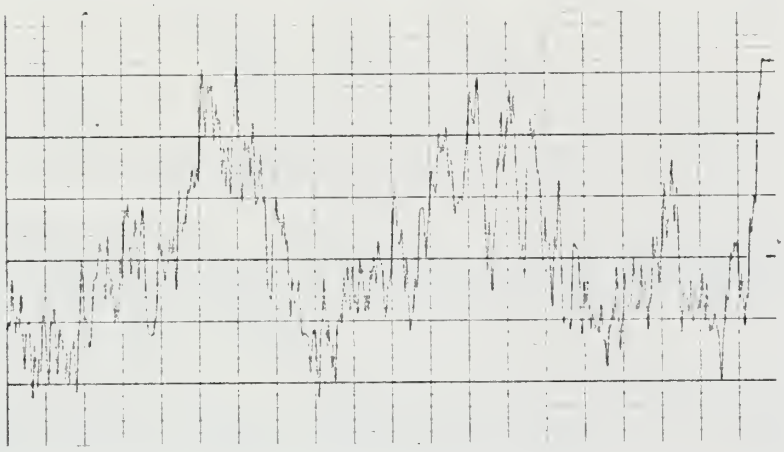

$Re = 12 \times 10^4$

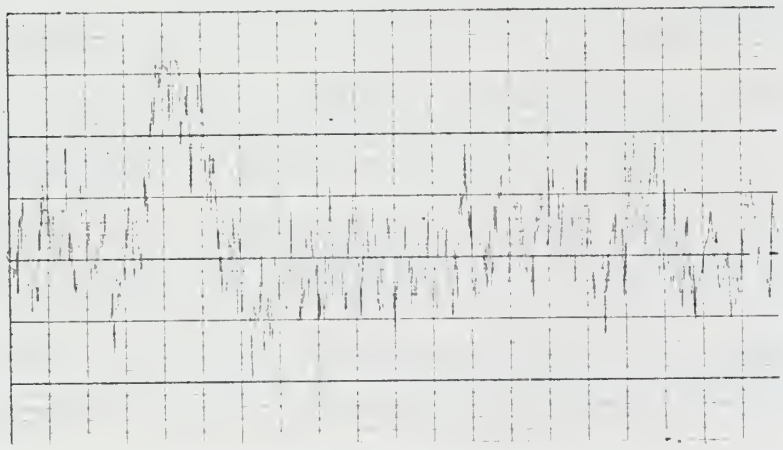

$R'e = 15 \times 10^4$

LIST OF REFERENCES

1. Smith, K. A., Merrill, H. S., Mickley, H. S., and Virk, P. S., "Anomalous Pitot Tube and hot film measurements in dilute poymer solutions," Chemical Engineering Science, v. 22, p. 619-26, 1967.

2. James, D. F., Laminar Flow of Dilute Polymer Solutions Around Circular Cylinders, PhD. Theses, California Institute of Technology, Pasadena, 1967.

3. Wetzel, J. M. and Tsai, F. Y., "Impact Tube Measurements in Dilute Polymer Solutions," AIChE Journal, v. 14, Nov. 4, p. 663-65, July 1968.

4. Strouhal, V., Ann. Physik Chem., v. 5, p. 216-51, 1878.

5. Goldstein, S., Modern Developments in Fluid Dynamics, v. 1, 2. Clarendon Press, 1938.

6. Lienhard, J. H., Synopsis of Lift, Drag and Vortex Frequency Data for Rigid Circular Cylinders, College of Eng. Research Div., Washington State University, Bulletin 300, 1966.

7. Morkovin, M. V., "Flow Around Circular Cylinder," Symposium on Fully Separated Flows, p. 102-18, 20 May 1964.

8. Wille, R., "Karman Vortex Streets," Advances in Applied Mechanics, v. 6, p. 273-87, Academic Press, 1960.

9. Marris, A. W., "A Review on Vortex Streets, Periodic Wakes, and Induced Vibration Phenomena," J. Basic Engineering, v. 86, p. 185-96, 1964.

10. Roshko,. A., "Experiments on Flow past a Circular Cylinder at very High Reynolds Numbers," J. Fluid Mech., v. 10, pt. 3, p. 345-56, 1961.

11. Delany, N. K. and Sorensen, N. E., Low Speed Drag of Circular Cylinders of Various Shapes, NACA TN 3038, 1953.

12. Roshko, A., On the Development of Turbulent Wakes from Vortex Streets, NACA Report 1191, 1954.

13. Roshko, A., On the Drag and Shedding Frequency of Two-Dimensional Bluff Bodies, NACA TN 3169, 1954.

14. Gaster, M., "Vortex Shedding from Slender Cones at Low Reynolds Numbers," J. Fluid Mech., v. 38, p. 565-76, 1969.

15. Humphreys, J. S., "On a Circular Cylinder in a Steady Wind at Transition Reynolds Numbers," J. Fluid Mech., v. 9, pt. 4, p. 603-12, 1960.

16. Bishop, R. E. D. and Hassan, A. Y., "The Life and Drag Forces on a Circular Cylinder in a Flowing Field," Proc. Roy. Soc., v. 277A, p. 32, 1964.

17. Wehrmann, O. H., "Influence of Vibration on the Flow Field Behind a Cylinder," Boundary Layers and Turbulence, Symposium on Boundary and Turbulence, including Geophysical Application, American Institute of Physics, 1967.

18. Gerrard, J. H., "The Three-Dimensional Structure of the Wake of a Circular Cylinder," J. Fluid Mech., v. 25, pt. 1, p. 143-64, 1966.

19. Sarpkaya, T. and Rainey, P. G., Flow of Dilute Polymer Solutions About Circular Cylinders, NPS-59SL1021A, 26 February 1971, Naval Postgraduate School, Monterey, California.

20. Patterson, R. W. Turbulent Flow Drag Reduction and Degration with Dilute Polymer Solutions, Div. of Eng. and Applied Physics, Eng. Sci. Lab., Harvard University, 1969.

21. Kudin, A. M. and Kalashinikov, V. N., "Karman Vortices in the Flow of Drag Reducing Polymer Solutions," Nature, v. 225, p. 445-46, January 1970.

22. Gadd, G. E., "Effects of Long Chain Molecular Additives in Water on Vortex Streets," Nature, v. 211, p. 169-70, 1966.

23. Gadd, G. E., "Effects of Drag Reducing Additives on Vortex Stretching," Nature, v. 217, p. 1040-42, March 1968.

24. Genstill, S. M., The Oscillatory Forces on a Semi-Submerged Circular Cylinder in Water and in Dilute Aqueous Solution of Poly(ethylene oxide), M. S. Thesis, Naval Postgraduate School, Monterey, June 1969.

25. Polyox Water-Soluable Resins, Union Carbide, 1968.

26. Hendricks, R. L., Flow of Dilute Polymer Solutions about Submerged Bodies, M. S. Thesis, Naval Postgraduate School Monterey, 1970.

27. Witter, R. C., Pressure Signatures of a Cylindrical Body Moving in Aqueous Solutions of Poly(ethylene oxide), M. S. Thesis, Naval Postgraduate School, Monterey, 1970.

28. Macousky, M. S., Vortex Induced Vibration Studies, David Taylor Model Basin, Rept. No. 1190, 1958.

INITIAL DISTRIBUTION LIST

		No. Copies
1.	Defense Documentation Center Cameron Station Alexandria, Virginia 22314	2
2.	Library, Code 0212 Naval Postgraduate School Monterey, California 93940	2
3.	Professor T. Sarpkaya, Code 59 Department of Mechanical Engineering Naval Postgraduate School Monterey, California 93940	1
4.	LT Richard E. Kell, USN Philadelphia Naval Shipyard Philadelphia, Pennsylvania 19112	1

Security Classification

DOCUMENT CONTROL DATA - R & D

(Security classification of title, body of abstract and indexing annotation must be entered when the overall report is classified)

ORIGINATING ACTIVITY *(Corporate author)*

Naval Postgraduate School
Monterey, California 93940

2a. REPORT SECURITY CLASSIFICATION

Unclassified

2b. GROUP

REPORT TITLE

The Effect of Dilute Polymer Solution on the Strouhal Frequency of Circular Cylinders

DESCRIPTIVE NOTES *(Type of report and inclusive dates)*

Degree of Mechanical Engineer; June 1971

AUTHOR(S) *(First name, middle initial, last name)*

Richard Edward Kell

REPORT DATE	7a. TOTAL NO. OF PAGES	7b. NO. OF REFS
June 1971	89	28

8. CONTRACT OR GRANT NO.	9a. ORIGINATOR'S REPORT NUMBER(S)
b. PROJECT NO.	
c.	9b. OTHER REPORT NO(S) *(Any other numbers that may be assigned this report)*
d.	

10. DISTRIBUTION STATEMENT

Approved for public release; distribution unlimited.

11. SUPPLEMENTARY NOTES	12. SPONSORING MILITARY ACTIVITY
	Naval Postgraduate School Monterey, California 93940

13. ABSTRACT

Flow of aqueous solutions of Polyox WSR-301, at a concentration of 25 wppm, was investigated in the cylinder drag transition region of Reynolds numbers. Frequency spectrum and drag force were measured on a circular cylinder (diameter 1 inch). Frequency spectrum, Strouhal frequency and drag force also were measured on circular cylinders in water (diameter 1 and 1-1/2 inch).

The polymer additive did not alter the vortex shedding frequency from that of water at the same Reynolds numbers. As the polymer degrades, a state is reached where concentration, Reynolds number and body size combination become such that the transition occurs in the boundary layer. Transition in the polymer solution occurred earlier than that in the pure solvent. At one Reynolds number, several regimes of flow may be observed as the polymer solution degrades.

DD FORM 1 NOV 65 1473 (PAGE 1)

S/N 0101-807-6811

Security Classification

KEY WORDS	LINK A		LINK B		LINK C	
	ROLE	WT	ROLE	WT	ROLE	WT
lymer flow						
uff Body						
rouhal Number						
rtex Shedding						
ircular cylinders in Polymer flow						
rouhal Frequency in Polymer flow						
rag Reduction						
ircular cylinder vortex shedding						
equency Spectrum of Circular cylinder wake						